A Review of Advanced Flexible Lithium-Ion Batteries

Tao Tao,* Shengguo Lu, and Ying Chen*

The rapid development of flexible electronics has triggered extensive efforts to explore matching flexible energy-storage devices as power sources. Flexible lithium-ion batteries (LIBs) have been demonstrated as the current most attractive and versatile energy storage devices for flexible electronics. A series of designs and constructions for flexible LIBs have been investigated in recent years. Particularly, significant progress has been achieved in finding high performance electrolyte and electrode materials, new structural designs, as well as suitable fabrication methods for flexible LIBs. In this review, the recent advances in the exploration of flexible lithium-ion batteries are summarized and discussed, with special focus on the selectivity of flexible electrode/electrolyte materials, cell structure design, and full cell assembly process. Perspectives for the future development of flexible LIBs are also discussed.

1. Introduction

Lithium-ion battery (LIB) offers the low cost, long cycle life, and high energy density, and is one of the most promising conversion and energy storage devices. A more recent advance in lithium-ion batteries (LIBs) is the development of flexible LIBs. Compared with conventional LIBs, flexible LIBs need to be foldable, lightweight, stretchable, and implantable, because of the requirement from portable and wearable electronic devices.[1]

Same as conventional LIBs, a flexible LIB also needs three main components: an electrolyte, an anode, and a cathode (**Figure 1**). Each component should be low cost, nontoxic, safe, lightweight, and bendable.[2] In addition, flexible electrodes must have low self-discharge, high capacity, stable cycling performance, and high rate capability. Polymer solid electrolytes employed as both electrolyte and separator need to possess high ionic conductivity, excellent mechanical flexibility, and high electrochemical stability.[3]

Full flexible LIBs as a new type of power source still show big challenges and prospects for study.[1,2] The challenge is to design and develop new electrode materials with impoved mechanical and electrochemical properties, and high safety performance under frequent mechanical deformation. Loading amount of active materials and electrolyte leakage are also the critical factors affecting the performance of the flexible LIBs. The reliable electrode materials require reasonable electrolytes, separators, and packaging materials to match. How to efficiently produce the flexible LIBs on a large scale to reduce their cost is the key. Tremendous efforts have been devoted to address these issues in recent years; however, the development of flexible LIBs remains in a preliminary stage. A reasonable selection, design, and optimization of new materials as well as cell fabrication technologies are yet to be explored.

Various functional materials (e.g., nanostructured silicon, metal oxide, metal sulfide, carbon, and their composites) and flexible solid polymer materials have been proposed as electrodes and electrolytes for flexible LIBs, respectively.[5,6] Carbonaceous materials including graphene, carbon cloth, carbon nanotubes (CNTs), carbon nanofibers (CNFs), and carbon papers are potential conductive substrates for flexible electrodes.[7,8] An electrochemical performance of flexible LIBs greatly depends on the selection and fabrication of suitable electrodes and electrolytes, as well as a rational configuration and design of cells.

Although several excellent reviews about flexible energy storage and conversion systems, including LIBs, supercapacitors, solar cells, and fuel cells, have been organized,[2,5–8] a comprehensive review regarding flexible LIBs has not yet been published since 2015. In this review, we mainly introduce the synthesis of various flexible electrodes as well as electrolytes, and their applications in flexible LIBs. Cell structure designs and configurations of flexible LIBs are also presented. Perspectives on the future development of flexible LIBs are provided, and the major challenges in this field are discussed.

Dr. T. Tao, Prof. S. G. Lu
School of Materials and Energy
Guangdong University of Technology
Guangzhou 510006, P. R. China
E-mail: taotao@gdut.edu.cn
Dr. T. Tao, Prof. Y. Chen
Institute for Frontier Materials
Deakin University
75 Pigdons Road, Waurn Ponds, VIC 3216, Australia
E-mail: ian.chen@deakin.edu.au

The ORCID identification number(s) for the author(s) of this article can be found under https://doi.org/10.1002/admt.201700375.

2. Flexible Electrodes

The design and fabrication of flexible electrodes are crucial for improving the performances of flexible LIBs. Comprehensively understanding the merits, drawbacks, and fabricating efficiency of flexible electrodes can benefit the practical application of flexible LIBs. A large range of electrodes have been developed to configure flexible LIBs. These electrodes usually consist of soft inorganic materials or organic materials embedded with a flexible substrate, or their composites, which are classified as anodes and cathodes. The next section will introduce the synthesis methods, fabrication technology, and structural design of flexible electrodes.
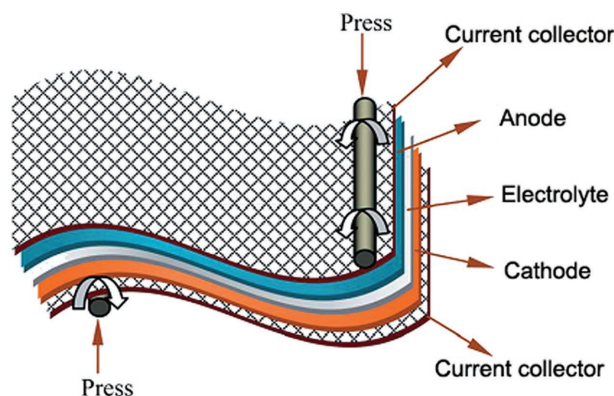
Figure 1. A schematic illustration of a full flexible LIB. Reproduced with permission.[4] Copyright 2012, Royal Society of Chemistry.

2.1. Anodes

Anode is a key component in LIBs. Several types of materials have been used in the anode for conventional LIBs, such as inorganic metallic compounds (A_xB_y; here A = Fe, Co, Ni, Mo, Sn, Mn, etc.; B = O, S, P, N), alloy materials (e.g., Si, Ge, Sn), and carbon based materials.[9,10] However, most of them are brittle materials and have a low elastic deformation limit, and thus are not suitable to be fabricated in the flexible LIBs. To overcome this issue, intrinsic bendable conductive supports (e.g., carbon nanofibers, graphene, carbon cloth, carbon nanotubes, and carbon papers), nonconductive flexible substrates (e.g., cotton, cloth, cellulose paper, and polymers), or low-dimensional nanostructured active materials with a high elastic limit are proposed as building blocks for preparing the flexible anodes.[11]

2.1.1. Carbon Nanofiber-Based Anodes

CNFs have a good electrical conductivity, a high surface area, excellent mechanical properties, and light weight, and have been employed as a free-standing and foldable substrate to fabricate flexible anodes.[12] A typical technology containing electrospinning and high temperature carbonization has been demonstrated to be one of the most efficient ways for producing CNFs (**Figure 2**a). Polyacrylonitrile (PAN) is used as the CNFs precursor. Although CNFs are in favor of improving the diffusion rate of Li^+ due to their large surface area, a low theoretical capacity limits their application in flexible anodes. In order to improve the electrochemical properties of flexible anodes, a series of CNFs-based anodes (**Table 1**), including porous CNFs,[12] P/CNFs,[13] CoO-graphene/CNFs,[14] Ge/CNFs,[15,16] MoS_2/CNF,[17–19] WO_x/CNFs,[20] MnO/CNFs,[21–23] SnO_x/CNFs,[24–26] SiO_x/CNFs,[27,28] Fe_3O_4/ CNFs,[29] $ZnxCo_{3-x}O_4$/CNFs,[30] NiS/CNFs,[31] SnO_x–ZnO/CNFs,[32] SnO_x/NiO/C,[33] Fe_2O_3–SnO_x/CNFs,[34] MoO_2–Mo_2C/CNFs,[35] $Li_4Ti_5O_{12}$/CNFs,[36] and TiO_2–Sn/CNFs[37] have been investigated (Figure 2b–h). An improved performance of these free-standing and binder-free flexible anodes is attributed to the combination of CNF supports and the active materials of high energy density. The CNFs conductivity framework with good mechanical properties can
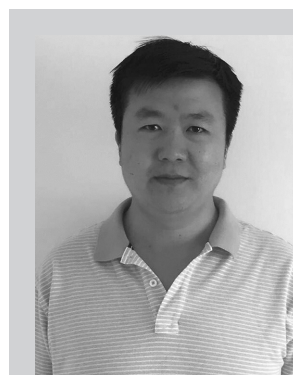
Dr. Tao Tao is currently an adjuct researcher at the Institute of Frontier Materials, Deakin University, Australia, and an associate professor at the School of Materials and Energy, Guangdong University of Technology, China. He obtained his B.Sc., Master's degree, and Ph.D. degree from Central South University, China and worked for over 3 years at the Institute for Frontier Materials at the Deakin University. Australia. His current research mainly focuses on the development of lithium batteries.

Prof. Shengguo Lu is currently a distinguished professor at the Guangdong University of Technology, and also a director of Guangdong Provincial Research Center on the Smart Materials and Energy Conversion Devices. Before joining the university, he was a senior research scientist consultant at the Strategic Polymer Sciences and an adjunct senior research associate at The Pennsylvania State University. Dr. Lu's research interest includes functional soft organic polymers, inorganic ceramics, organic–inorganic composites, and their applications as sensors, actuators, energy storages, and electrocaloric refrigerators.

Prof. Ying Chen is an Alfred Deakin Professor and the Chair in Nanotechnology at Deakin University, Australia. He received his B.Sc. from Tsinghua University in China and Ph.D. degree from University of Paris Sud, France. Professor Chen has worked for 15 years at the Australian National University in Canberra and then joined Deakin University in 2009. His current research focuses on the synthesis of a variety of nanomaterials including boron nitride nanotubes and nanosheets, graphene, and nanoparticles, and their applications in batteries, supercapacitors, environmental protection, and medical applications.

efficiently alleviate the volume change caused in the active materials during cycling.

Porous CNFs are employed as flexible anodes in LIBs because of their special 3D porous structure which can shorten
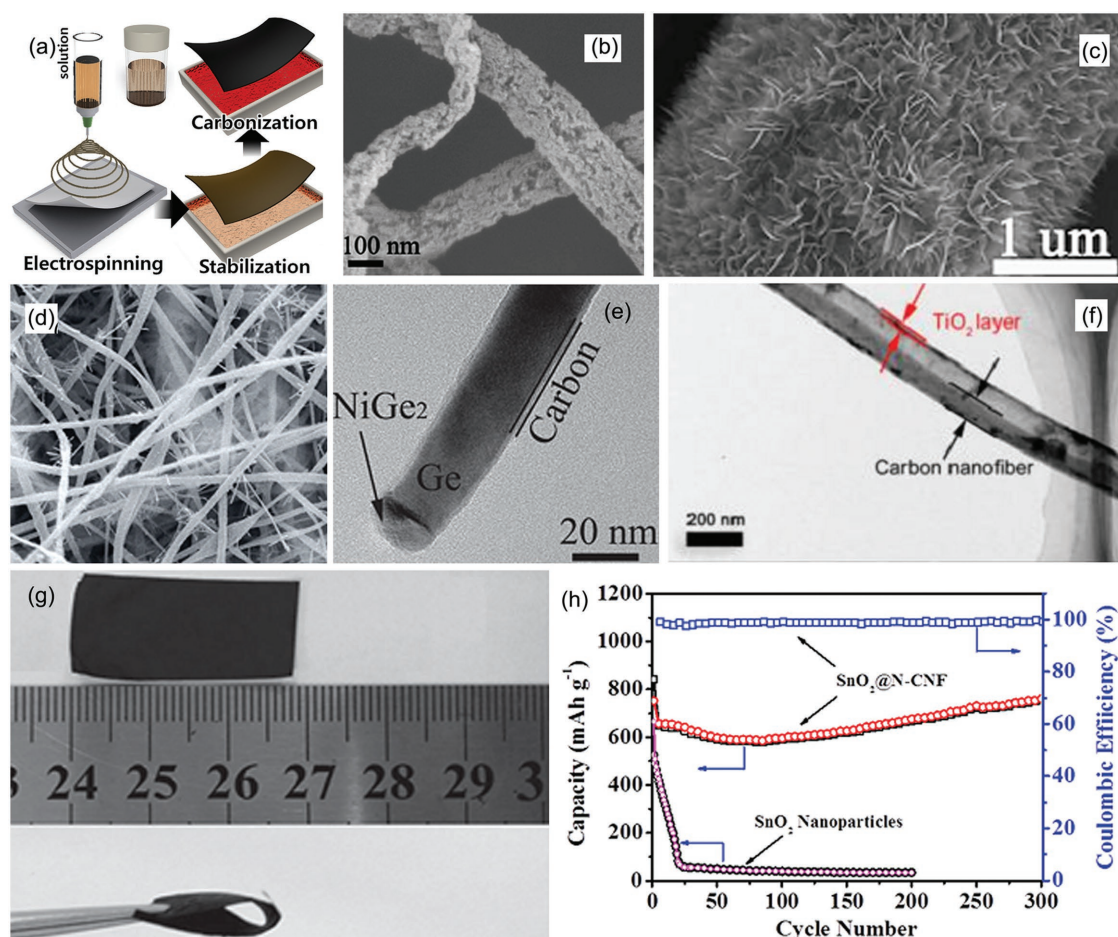
**ADVANCED
SCIENCE NEWS**

www.advancedsciencenews.com

**ADVANCED
MATERIALS
TECHNOLOGIES**

www.advmattechnol.de

Figure 2. a) Electrospinning process for preparing flexible CNFs. b) High magnification scanning electron microscope (SEM) image of CNFs. c) SEM image of the hierarchical MoS_2/active carbon fiber cloth composites. d,e) SEM image and transmission electron microscopy (TEM) image of carbon–GeNWs–CNFs composite. f) SEM image of pipe-wire TiO_2–Sn@CNF. g,h) Photograph and cycling performance (1 A g^{-1}) of the flexible SnO_2@N-CNF film. a) Reproduced with permission.[23] Copyright 2017, Elsevier. b) Reproduced with permission.[12] Copyright 2015, Elsevier. c) Reproduced with permission.[17] Copyright 2014, Royal Society of Chemistry. d,e) Reproduced with permission.[16] f) Reproduced with permission.[37] Copyright 2017, American Chemical Society. g,h) Reproduced with permission.[26]

the diffusion distance of lithium ions between electrode and electrolyte and improve the electrical conductivity of CNF anodes.[12] A combination method based on an electrospinning technology and a two-step carbonization process is proposed to synthesize the flexible and binder-free porous CNF anodes. A plenty of micro/mesopores in CNFs can be formed during the second carbonization process at 1000 °C in argon and air gas mixture. The porous CNFs as self-supported and binder-free flexible anodes for LIBs show a high reversible capacity (1780 mAh g^{-1} at 50 mA g^{-1} after 40 cycles) and good cycling performance (1550 mAh g^{-1} at 500 mA g^{-1} after 600 cycles). Moreover, porous CNFs are used as substrates to fabricate a self-supported and flexible anode for LIBs. The porous CNFs can alleviate the volume change and enhance the electrical conductivity of active materials during cycling. A flexible integrated anode consisting of crystalline red P and porous CNFs exhibits an outstanding reversible capacity of 2030 mAh g^{-1} at 260 mA g^{-1} after 100 cycles.[13]

Thin MoS_2 nanosheets incorporated with CNFs are also prepared as flexible anodes for LIBs with high electrochemical

properties via the electrospinning method followed by the carbonization and the solvothermal reaction.[17] The obtained anodes have an excellent flexible structure, because both CNFs and MoS_2 nanosheets are flexible. In order to further improve the mechanical properties and conductivity of flexible CNFs-based anodes, graphene with excellent conductive and mechanical properties is used as additive for constructing these hybrid anodes. Flexible anodes composed of CoO/graphene/CNFs are prepared by electrospinning and subsequent heating treatment, which show high electrochemical performances.[14] After 352 cycles, their reversible capacity at a current density of 500 mA g^{-1} can be stabilized at 690 mAh g^{-1}. A similar method consisting of reducing, electrospinning, and thermal treatment is developed to fabricate a flexible anode of SnO_x/graphene/CNFs for LIBs.[24] It is believed that graphene and CNFs are favorable to protect the tin oxides nanoparticles during Li alloying and dealloying.

A vapor–liquid–solid growth method has been proposed to prepare a flexible anode of carbon coated Ge nanowires (NWs)/CNFs for LIBs.[16] The polymer nanofibers (polyacrylonitrile/nickel

Table 1. Typical CNF based anode materials used in LIBs.

Materials	Synthesis process	Test condition	Performance	Ref.
Red phosphorus/CNFs	Electrospinning + carbonization	Coin cell/0.001–2.5 V	2030 mAh g^{-1}/100 cycles/260 mA g^{-1}	[13]
CoO/graphene/CNFs	Electrospinning + thermal treatment	Coin cell/0.001–3 V	690 mAh g^{-1}/352 cycles/500 mA g^{-1}	[14]
Germanium/CNFs	Electrospinning + thermal treatment	Coin cell/0.005–1.2 V	1420 mAh g^{-1}/100 cycles/244 mA g^{-1}	[15]
MoS$_2$ nanosheet/CNFs	Sonication + thermal treatment	Coin cell/0.005–3 V	418 mAh g^{-1}/200 cycles/500 mA g^{-1}	[17]
Tungsten oxide/CNFs	Electrospinning + thermal treatment	Coin cell/0.001–3 V	321 mAh g^{-1}/85 cycles/50 mA g^{-1}	[20]
MoS$_2$ nanoflakes/CNFs	Electrospinning + carbonization	Coin cell/0.005–3 V	1150 mAh g^{-1}/100 cycles/50 mA g^{-1}	[18]
Fe$_3$O$_4$/CNFs	Hydrothermal + carbonization	Coin cell/0.005–3 V	754 mAh g^{-1}/100 cycles/100 mA g^{-1}	[38]
Germanium nanowires/CNFs	Situ vapor–liquid–solid	Coin cell/0.005–1.2 V	1520 mAh g^{-1}/80 cycles/100 mA g^{-1}	[16]
Porous CNFs	Electrospinning + two-step carbonization	Coin cell/0.001–3 V	1550 mAh g^{-1}/600 cycles/500 mA g^{-1}	[12]
MoS$_2$/porous CNFs	Electrospinning + carbonization + the solvothermal reaction	Coin cell/0.01–3 V	736 mAh g^{-1}/50 cycles/50 mA g^{-1}	[19]
Sn/CNFs	Electrospinning + thermal treatment	Coin cell/0.01–3 V	350 mAh g^{-1}/200 cycles/200 mA g^{-1}	[25]
Si/SiO$_2$/CNFs	Electrospinning + thermal treatment + chemical vapor deposition	Coin cell/0.01–2 V	733 mAhg^{-1}/50 cycles/100 mA g^{-1}	[39]
Si/CNFs	Electrospinning + carbonization	Coin cell/0.01–2 V	1045 mAh g^{-1}/20 cycles/100 mA g^{-1}	[27]
MnO/CNFs	Electrospinning + thermal treatment	Coin cell/0.01–3 V	987 mAh g^{-1}/150 cycles/100 mA g^{-1}	[21]
SnO$_x$/graphene/CNFs	Electrospinning + thermal treatment	Coin cell/0.005–3 V	545 mAh g^{-1}/1000 cycles/200 mA g^{-1}	[24]
Fe$_2$O$_3$ nanoshells/CNFs	Impregnation + thermal treatment	Coin cell/0.2–3 V	1135 mAh g^{-1}/200 cycles/400 mA g^{-1}	[40]
Zn$_x$Co$_{3-x}$O$_4$ nanocubes/CNFs	Hydrothermal process + thermal treatment	Coin cell/0.01–3 V	600 mAh g^{-1}/300 cycles/400 mA g^{-1}	[30]
NiS/CNFs	Electrospinning + carbonization	Coin cell/0.01–3 V	1149 mAh g^{-1}/100 cycles/100 mA g^{-1}	[31]
SnO$_2$/N-doped CNFs	Electrospinning + carbonization	Coin cell/0.01–3 V	754 mAh g^{-1}/300 cycles/1 A g^{-1}	[26]
SnO$_x$/ZnO/CNFs	Electrospinning + annealing	Coin cell/0–3 V	963 mAh g^{-1}/55 cycles/100 mA g^{-1}	[32]
MnO microparticles/CNFs	Electrospinning + carbonization + hydrothermal method	Coin cell/0.001–3 V	984 mAh g^{-1}/100 cycles/200 mA g^{-1}	[22]
SnO$_2$/NiO/CNFs	Electrospinning + carbonization	Coin cell/0.05–3 V	675 mAh g^{-1}/100 cycles/100 mA g^{-1}	[33]
MnO nanocrystals/CNFs	Electrospinning + carbonization	Coin cell/0.01–3 V	923 mAh g^{-1}/90 cycles/123 mA g^{-1}	[23]
Foldable CNFs	Electrospinning + peroxidation + carbonization	Coin cell/0.01–3 V	630 mAh g^{-1}/100 cycles/200 mA g^{-1}	[41]
Fe$_2$O$_3$/SnO$_x$/CNFs	Impregnation + thermal treatment	Coin cell/0.01–3 V	756 mAh g^{-1}/55 cycles/100 mA g^{-1}	[34]
MoO$_2$/Mo$_2$C/CNFs	Impregnation + thermal treatment	Coin cell/0.01–3 V	1098 mAh g^{-1}/70 cycles/100 mA g^{-1}	[35]
Pipe-wire TiO$_2$/Sn/CNFs	Electrospinning + atomic layer deposition	Coin cell/0.01–3 V	643 mAh g^{-1}/1100 cycles/200 mA g^{-1}	[37]

acetate/tetramethoxygermane) are first synthesized by using electrospinning, then heated at 280 °C in air for 3 h to stablize the 3D nanofiber structure, and finally carbonized at 550 °C in Ar/H$_2$ atmosphere for growing carbon-coated Ge nanowires on the surface of CNFs. The novel in situ vapor–liquid–solid process is expected to design the self-supported and flexible electrodes of LIBs with high performances. A hydrothermal method followed by carbonization is another way to fabricate a flexible nano-Fe$_3$O$_4$/bacterial cellulose (BC) hydrogels-CNFs anode for LIBs.[29] In this process, BC is used as a carbon precursor to prepare the flexible CNF matrix because it is cheap and nontoxic. The obtained paper-like nano-Fe$_3$O$_4$/BC-CNF composites can be employed as free-standing and binder-free anodes without extra conductive additives. SnO$_2$ nanoparticles imbedded in the nitrogen-doped CNFs are prepared via a novel electrospinning strategy.[26] An electrospinning-liquid precursor contains pyromellitic dianhydride, 4,4′-oxydianiline, N,N-dimethylformamide, and SnCl$_2$•2H$_2$O. After electrospinning and carbonization, the obtained SnO$_2$@N-CNF materials show

good flexibility and excellent structural stability. An integrated strategy including electrospinning and atomic layer deposition (ALD) has been developed to build pipe-wire TiO$_2$–Sn@CNFs flexible anode for LIBs.[37] The nanosized Sn can be uniformly anchored on carbon nanofibers by electrospinning. ALD techniques are used to coat a thin protecting layer of TiO$_2$ onto the Sn@CNFs surface. The pipe-wire anode makes full use of advantages of TiO$_2$, Sn, and CNFs, and shows superior electrochemical performances.

As discussed above, it has been demonstrated that CNF based anodes are more suitable for developing flexible LIBs because of their low cost, light weight, high chemical stability, and good mechanical property. CNFs can provide free space to load high capacity active materials, alleviate their volume expansion, promote electron transfer, and maintain the structural stability of electrodes during cycling. Although a lot of research work has been done in this field, deep understanding of systematic mechanism for designing the CNFs based anodes is still very crucial in the development of future flexible LIBs.
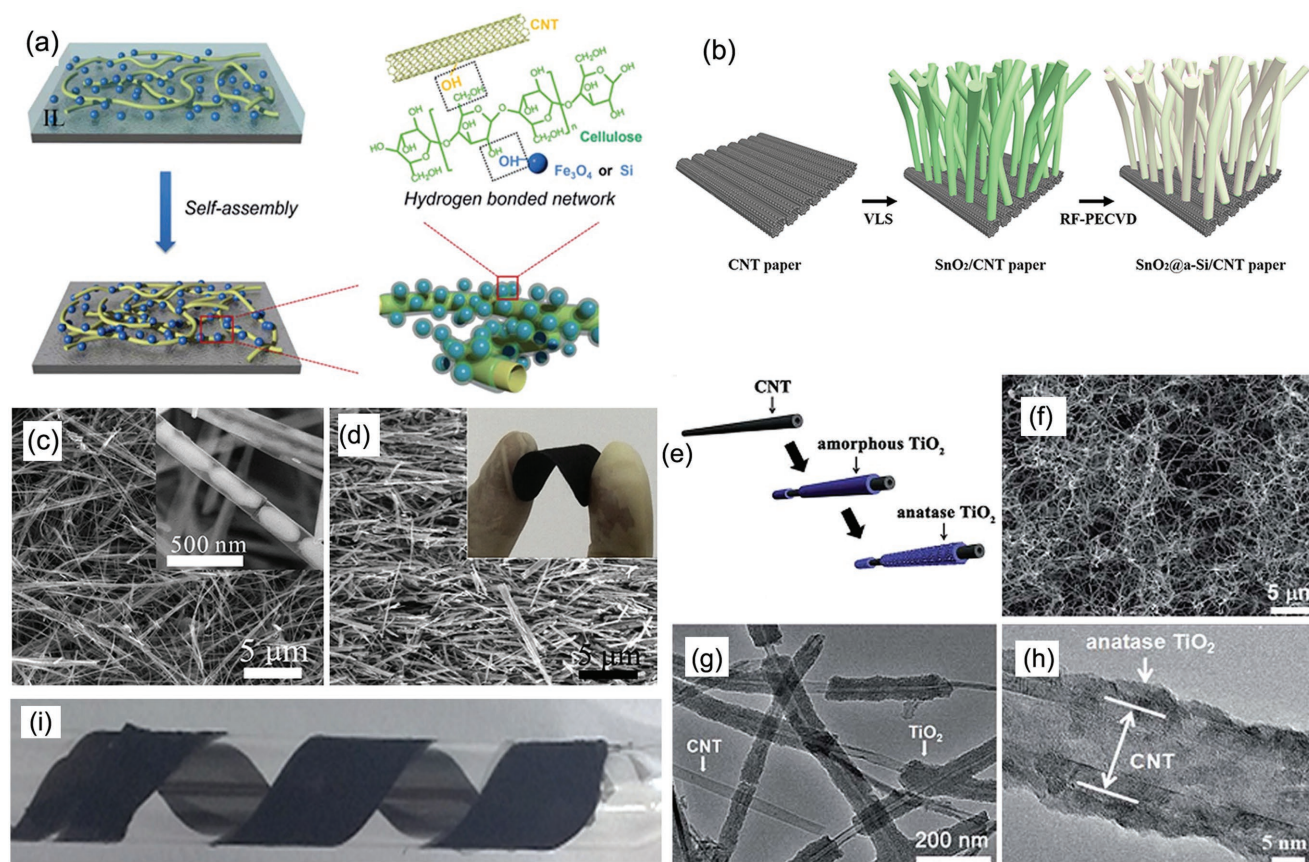
Figure 3. a) In situ regenerating process for fabricating the nanoparticle (NP)/CNT composites. b) Schematic illustrating the steps followed to synthesize the SnO_2@a-Si core–shell on CNT paper. c) SEM images of the V_2O_3@C NWs film and d) corresponding digital picture. e) Illustration of the microstructure evolution of anatase TiO_2/CNT core–shell structures. f) Low magnification SEM image of amorphous TiO_2/CNT sponges, and g,h) TEM images of TiO_2 layer coated CNTs and an individual anatase TiO_2/CNT. i) A digital picture of wound CNT films on a round bar. a) Reproduced with permission.[45] Copyright 2017, Royal Society of Chemistry. b) Reproduced with permission.[42] Copyright 2017, IOP Publishing Ltd. c,d) Reproduced with permission.[50] Copyright 2016, Elsevier. e–h) Reproduced with permission.[47] Copyright 2016, Royal Society of Chemistry. i) Reproduced with permission.[56] Copyright 2015, Elsevier.

Additionally, compared with CNTs, CNFs have a significant advantage of the low cost and two major shortcomings for constructing flexible electrodes: much less functional groups and low surface specific areas. Less functional groups lead to a weak interfacial bonding between CNFs and active materials, and low specific surface area results in low conductivity and carrying capacity of active materials. Therefore, developing new CNFs with more functional groups and high surface specific areas is expected to further improve their application in the design and fabrication of flexible LIBs.

2.1.2. Carbon Nanotube-Based Anodes

CNTs and their composites have extensively been investigated both as foldable substrates and active materials to prepare free-standing anodes for flexible LIBs due to their excellent conductivity (103 S cm^{-1}), good mechanical properties, and high surface area (1600 m^2 g^{-1}). Several good review papers have focused on how to design and fabricate various kinds of CNT based anodes for flexible LIBs.[2,7,9] This section will mainly introduce the recent advances in this field.

A variety of techniques have been developed to build CNT based free-standing anodes for flexible LIBs (**Figure 3** and **Table 2**), including vacuum filtration,[42] chemical vapor deposition (CVD),[43] solvothermal method,[44] in situ regenerating,[45] and drop-casting.[46] For example, a 3D free-standing CNT anode has been employed to fabricate a flexible LIB.[49] First, CNTs are grown on a Cu substrate via catalytic thermal CVD, and then transferred onto a graphene–polyethylene terephthalate film at 90 °C by a thermal lamination process for preparing the flexible anode. The obtained 3D free-standing CNT anode shows an improved areal capacity (0.25 mAh cm^{-2}). Coaxial TiO_2/CNT composite sponges as a high-performance anode for flexible LIBs are synthesized by three steps: in situ hydrolysis, freeze-drying, and thermal annealing.[47] These composite sponges have high pressure-resistance, conductivity, and porosity. Coating of a thin TiO_2 layer on the surface of CNTs can improve the compressive strength and structural stability of CNTs framework. SnS_2/CNT sponges have been proposed as binder-free and free-standing anodes for flexible LIBs.[48] High electronic conductivity CNT sponges as excellent 3D porous flexible substrates are prepared via chemical vapor deposition. Nanostructured SnS_2 active materials are embedded in CNT

Table 2. Carbon nanotube-based flexible anodes used in LIBs.

Materials	Synthesis process	Test condition	Performance	Ref.
1T-MoSe$_2$/CNTs	One-step solvothermal method	Coin cell/0.01–3 V	971 mAh g^{-1}/100 cycles/300 mA g^{-1}	[44]
Si nanoparticles/CNTs	In situ regenerating	Coin cell/0.005–3 V	1075 mAh g^{-1}/60 cycles/300 mA g^{-1}	[45]
SnO$_2$@Si core–shell nanowires/CNTs	Vacuum filtration method	Coin cell/0.05–2 V	892 mAh g^{-1}/25 cycles/5.2 mAh cm^{-2}	[42]
Cd$_2$GeO$_4$ nanowire/graphene oxide/CNTs	Hydrothermal process + filtration	Coin cell/0.01–3 V	784 mAh g^{-1}/30 cycles/200 mA g^{-1}	[54]
CoSnO$_3$/graphene/CNTs	Filtration + annealing	Coin cell/0.005–3 V	1098.7 mAh g^{-1}/150 cycles/100 mA g^{-1}	[55]
Coaxial TiO$_2$/CNTs	In situ hydrolysis method	Coin cell/0.01–3 V	221 mAh g^{-1}/100 cycles/100 mA g^{-1}	[47]
SnS$_2$/CNTs	Solvothermal method	Coin cell/0.01–3 V	502 mAh g^{-1}/100 cycles/100 mA g^{-1}	[48]
Li$_4$Ti$_5$O$_{12}$/ CNTs	Solution-based method + heat treatment	Coin cell/1–2.5 V	165 mAh g^{-1}/400 cycles/1724 mA g^{-1}	[51]
V$_2$O$_3$ nanorods/ CNTs	Hydrothermal method + annealing	Coin cell/0–3 V	186 mAh g^{-1}/125 cycles/100mAg^{-1}	[50]
CNT films	Chemical vapor deposition and spinning	Coin cell/0.01–2 V	446 mAh g^{-1}/50 cycles/100 mA g^{-1}	[56]
Li$_4$Ti$_5$O$_{12}$/CNTs/cellulose nanofiber	Pressure-controlled aqueous extrusion process	Coin cell/1–2.5 V	134 mAh g^{-1}/500 cycles/1750 mA g^{-1}	[52]

sponges substrates through a solvothermal method. Compared with pure CNT sponges, the SnS$_2$/CNT sponges show a higher areal capacity. A flexible anode of ultralong peapod-like V$_2$O$_3$ encapsulated with CNT nanowires is fabricated via a hydrothermal treatment followed by annealing for 4 h at 600 °C in Ar/H$_2$.[50] In this anode, CNTs can provide sufficient space to restrain the aggregation and dissolution during cycling, resulting in its high performance.

A framework of aligned CNTs with high flexibility and conductivity is used to support a free-standing anode,[51] which is synthesized by a CVD process. Mesoporous lithium titanate (LTO) nanoclusters are loaded into this framework via a two-step process (a solution-based method and heat treatment in air) for preparing LTO/CNT composites. The obtained LTO/CNT composite can serve as the free-standing and binder-free anodes. The mesoporous LTO nanoclusters with interconnected porous structures can guarantee active materials to be close to the conductive framework and the electrolyte. A hybrid film consisting of CNTs, carbonized CNF, and LTO is proposed as a paper anode for LIBs, which is constructed via a two-step fabrication process containing a pressured extrusion papermaking method and in situ carbonization under Ar.[52] By this process, LTO nanoparticles are well embedded into the 3D porous C-CNF/CNTs network to form the paper anode. The lightweight, flexible, and free-standing paper anodes with high conductive and structural stability exhibit excellent cycling and rate performance.

A new method involving in situ regenerating a mixture of active nanoparticles, CNTs, and cellulose in water has been developed for building a flexible anode of LIBs.[45] The cellulose acts as a binder of anodes to facilitate the interfacial contacts between CNTs and active nanoparticles. Also, the cellulose with hydroxyl groups has regenerative and self-healing functions, which can maintain the architecture stability of anodes and enable stable cycling. A solvothermal method is reported for designing hierarchical nanostructure of single-walled carbon nanotubes (SWCNTs) and 1T-MoSe$_2$ composite as a flexible anode for LIBs.[53] The 1T-MoSe$_2$ nanosheets possess an expanded interlayer spacing of 10.0 Å, and SWCNTs are oxidized in air to generate the oxygen groups. During the synthesis process, the functional oxygen groups of SWCNTs can interact with the edge Mo of 1T-MoSe$_2$ nanosheets to

form Mo—O—C bonds, which work as bridge to connect the 1T-MoSe$_2$ nanosheets and the SWCNTs substrate for fabricating a hierarchical nanostructure.

Generally, CNT-incorporated anodes can be categorized into two types: (1) innerimplantation: active materials embedded into the inner space of hollow CNTs; (2) outerdeposition: active materials bonded on the outer surface of CNTs. In comparison with outer deposition, active materials are adhered on the internal surface of CNTs, and have a good contact with them, which can efficiently suppress the volume expansion of the inner implanted active materials and resist their detachment from the CNTs. Whereas, outerdeposited materials have direct access to the electrolyte and keep from the direct contact of CNTs with it, easily leading to a poor electrochemical performance of the composite electrode because of the formation of an unstable solid electrolyte interface film during cycling. Therefore, the innerimplantation is a better way to synthesize CNT-incorporated flexible anodes.

Employing CNT networks in fabricating flexible anode materials has several obvious advantages: (1) high surface area and chemical stability maintain the integrity of electrode structure during cycling; (2) good electrical conductivity ensures an enhanced electrochemical reaction kinetics of the anode; (3) good flexibility suppresses the volume change of electrode materials. However, a right mass loading of high-capacitance active materials on CNTs could be required, because developing high performance CNT-based flexible anode needs to address the effects of capacity and the electrical conductivity. Also, residual metallic impurities in CNTs could be a problem, which would influence the overall performance of the composite electrodes. These issues as well as its high cost should limit the future development of CNT-based flexible anode.

2.1.3. Graphene-Based Anodes

Graphene, one-atom-thick 2D sp^2-bonded carbon sheet, has a high theoretical specific surface area (about 2630 m^2 g^{-1}), excellent mechanical flexibility, high electrical conductivity, good thermal conductivity, excellent chemical stability, and low installation cost. These outstanding properties enable graphene
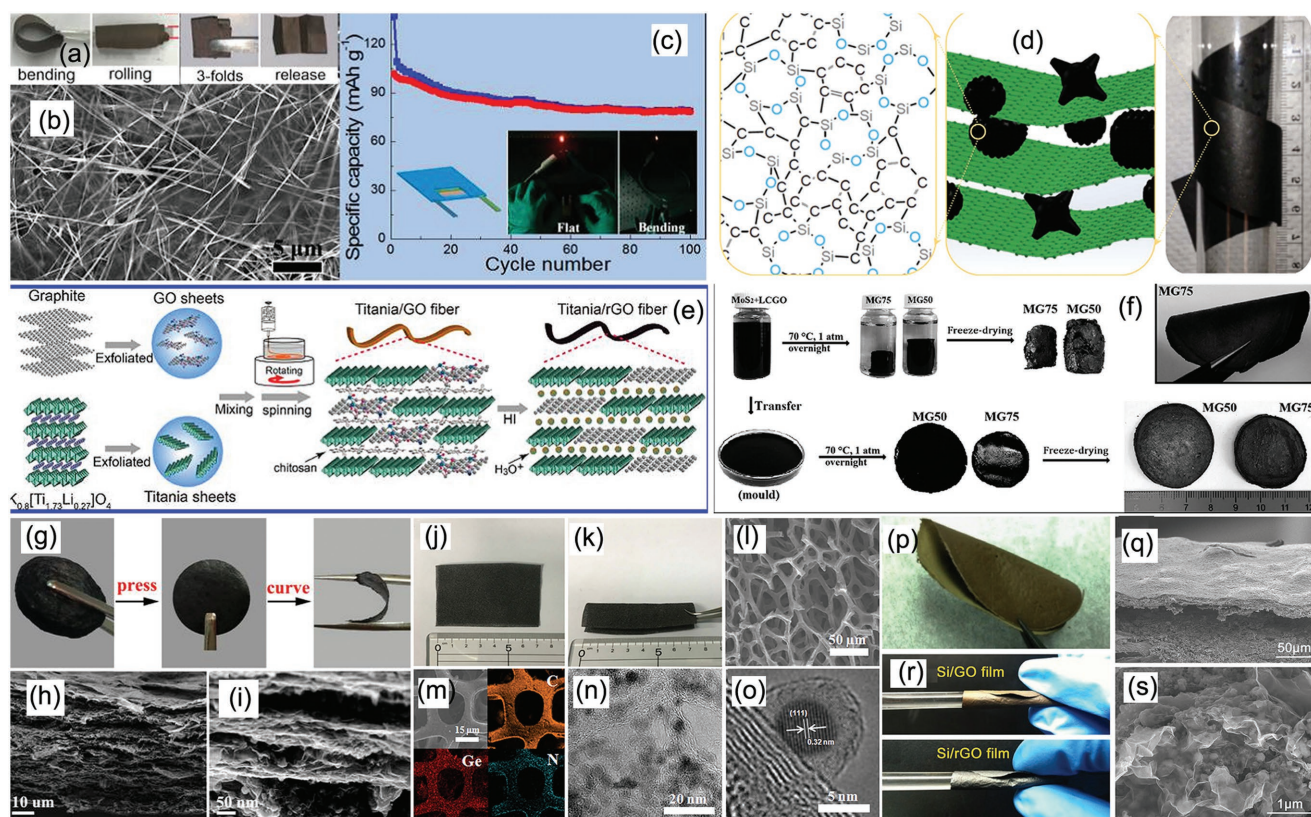
Figure 4. a) Digital photos illustrating the flexibility and foldability states and b) SEM image of the rGO/Mn_3O_4 membrane. c) 3D schematic configuration and cycling performance of a flexible full battery (rGO/Mn_3O_4||$LiMn_2O_4$), and optical images on a red light emitting diode (LED) powered by the battery under flat and bending states. d) Digital photo and schematic illustration of proposed hybrid structure of the freestanding paper along with the atomic structure of pyrolyzed SiOC particle. e) Schematic illustrating the steps followed to fabricate the titania/rGO composite. f) Schematic procedure to fabricate flexible MoS_2-reduced graphene oxide (MG) composite hydrogels. g) Schematic procedure to prepare a flexible binder-free 3dimensional graphene (DG)/Fe_2O_3 electrode, and h,i) its SEM image of the side-view and high-magnification SEM image of the interior microstructure. j,k) Digital photos. l) SEM image and m) Energy dispersive X-ray spectrometry (EDS) elemental maps of Ge, C, and N, respectively, and n,o) TEM images of a flexible Ge-quantum dot (QD)@ nitrogen-doped graphene (NG)/nitrogen-doped graphene foam (NGF) yolk–shell nanoarchitecture. p,r) Digital photos of Si/rGO flexible film in bending states. q,s) SEM images (low- and high-magnification) of Si/rGO films. a–c) Reproduced with permission.[63] Copyright 2016, American Chemical Society. d) Reproduced with permission.[65] Copyright 2016, Nature Publishing Group. e) Reproduced with permission.[71] Copyright 2017, American Chemical Society. f) Reproduced with permission.[67] g–i) Reproduced with permission.[70] Copyright 2017, American Chemical Society. j–o) Reproduced with permission.[74] Copyright 2017, Nature Publishing Group. p–s) Reproduced with permission.[60] Copyright 2016, Elsevier.

to be an excellent material for fabricating the flexible anodes. However, graphene-based anode often struggles with its low theoretical capacity, large initial irreversible capacity, and fast capacity fading during cycling, therefore incorporating high-capacitance inorganic active materials on the flexible graphene matrix is necessary. The synthesis of graphene and its composite based flexible anodes and their applications in LIBs over the past years have been well summarized.[57–59] This part will present a brief overview on the development of various graphene based flexible anodes for LIBs in the past two years (from 2016 to 2017).

Various types of graphene/high-capacitance active material (e.g., Si,[60] Co_3O_4,[61] $Mn_2P_2O_7$,[62] Mn_3O_4,[63,64] SiOC,[65] MoS_2,[66,67] Ge@TiO_2,[68] SiO,[69] Fe_2O_3,[70] TiO_2,[71] Fe_7Se_8,[72] copper silicate[73]) composites have been explored as flexible anode materials for LIBs (**Figure 4** and **Table 3**). A flexible hybrid film of Si/reduced graphene oxide (mass ratio of 3:7) has been fabricated via a magnesiothermic reduction at 650 °C for 2 h followed by layer-by-layer assembly process.[60] The

resulting hybrid film as a LIB anode shows an enhanced electrochemical performance, which could be attributed to the synergies of Si hollow nanosheets and reduced graphene oxide. It has been expected that a $Mn_2P_2O_7$–carbon@reduced graphene oxide composite paper may be a feasible choice for high performance flexible LIB anode.[62] First, Mn^{2+} ions are absorbed by the bacteria, mixed with a graphene oxide solution, filtered by vacuum filtration, and annealed for 2 h at 700 °C to form the micro-yolk–shell $Mn_2P_2O_7$–carbon@reduced graphene oxide composite paper. A SiOC particles/graphene composite paper synthesized by a vacuum filtration process has been proposed as a flexible anode for LIBs.[65] SiOC particles have excellent Li intercalation capacity and high thermodynamic and chemical stability, which ensures the high electrochemical performance and low volumetric changes of electrode. The porous graphene matrix offers high electrical conductivity and structural stability, serving as an excellent conductive current collector.

A scalable wet-spinning strategy has been suggested to fabricate a new type of wire-shaped LIB anode composed of titania

Table 3. Graphene based flexible anodes used in LIBs.

Materials	Synthesis process	Test condition	Performance	Ref.
Si/rGO hybrid film	Layer-by-layer assembly process	Coin cell/0.005–2 V	650 mAh g^{-1}/150 cycles/200 mA g^{-1}	[60]
Mn$_2$P$_2$O$_7$–carbon@reduced graphene oxides papers	In situ synthesize + vacuum filtration process	Coin cell/0.01–3 V	400 mAh g^{-1}/2000 cycles/5000 mA g^{-1}	[62]
Graphene/Mn$_3$O$_4$ nanocomposite membranes	Modified Hummer's method + vacuum filtration	Coin cell/0.005–3 V	802 mAh g^{-1}/100 cycles/100 mA g^{-1}	[63]
Porous Mn$_3$O$_4$ nanorod/reduced graphene oxide hybrid paper	Vacuum filtration + thermal treatment	Coin cell/0.05–3 V	573 mAh g^{-1}/100 cycles/100 mA g^{-1}	[64]
Silicon oxycarbide glass/graphene composite paper	Vacuum filtration	Coin cell/0.01–2.5 V	588 mAh g^{-1}/1020 cycles/1600 mA g^{-1}	[65]
Layered MoS$_2$/graphene nanosheets	One-pot hydrothermal method	Coin cell/0.05–3 V	870 mAh g^{-1}/200 cycles/1000 mA g^{-1}	[66]
3D N-graphene foam/Ge quantum dot/N-graphene nanoarchitecture	CVD + hydrothermal process + annealing + acid etching	Coin cell/0.01–1.5 V	1220 mAhg^{-1}/1000 cycles/1600 mA g^{-1}	[74]
3D graphene/Fe$_7$Se$_8$@C	One-step calcination method	Coin cell/0.01–3 V	884 mAh g^{-1}/120 cycles/100 mA g^{-1}	[72]
3D MoS$_2$/reduced graphene oxide	Spontaneous self-assembly process + freeze-drying	Coin cell/0.01–3 V	450 mAh g^{-1}/500 cycles/400 mA g^{-1}	[67]
Cauliflower-like FeS$_2$/graphene foam	One-pot hydrothermal method	Coin cell/0.05–3 V	1080 mAh g^{-1}/100 cycles/178 mA g^{-1}	[75]
Fe$_2$O$_3$ nanoframeworks/graphene	Self-assembly + confined Ostwald ripening strategy	Coin cell/0.01–3 V	1129 mAh g^{-1}/130 cycles/200 mA g^{-1}	[70]

sheets molecularly embedded in reduced graphene oxide.[71] The new anode shows an excellent mechanical flexibility and high battery property. A 3D porous flexible anode consisting of atomically thin 2D MoS$_2$ encapsulated within reduced graphene oxide has been successfully fabricated via a spontaneous self-assembly and subsequent freeze-drying process.[67] It is believed that the method is low cost and readily scalable, and can be extended to prepare multifunctional flexible electrodes. 3D graphene/Fe$_7$Se$_8$@C nanocomposites have been proposed as excellent flexible anode materials, which are synthesized by one-step calcination of 3D graphene/metal organic framework with Se powder under Ar/H$_2$ flow for 2 h at 600 °C.[72] A facile and general strategy has been developed to produce 3D interconnected porous nitrogen-doped graphene foam with encapsulated Ge quantum dot/nitrogen-doped graphene yolk–shell nanoarchitecture,[74] which can be served as a high performance flexible anode of LIBs. The strategy includes CVD, hydrothermal process, annealing, and acid etching. The obtained special 3D interconnected yolk–shell nanoarchitecture affords internal void space to suppress the volumetric changes of Ge during lithiation, and offers numerous open channels to favor the fast electron and lithium ion diffusion.

Despite graphene-based binder-free anodes for LIBs show high electrochemical performances, several issues still remain to be addressed. In most cases, the graphene content in composite anode material is relatively higher (>10%). Too much graphene often results in a lower specific volumetric capacity of the electrodes because of its poor density and porous structure. Therefore, the graphene content in composite anode material should be decreased in future work under the premise of ensuring the electrochemical performance of flexible anodes. Also, the defect concentration of artificial graphene is very high, which can lower the electrical conductivity of anode and affect Li-ion diffusion. Thus, how to coordinate and balance the relation between the defect concentration, the ion diffusion process, and the conductivity should be considered in future studies. Third, the interfacial contact between the graphene

and the active materials is critical to the electrochemical performance and mechanical properties of binder-free graphene-based anodes. Without binder, their contact strength on each other is relatively weak. Therefore, further improvement of their mechanical strength and contact strength is very important to practical application. Moreover, the industrialization of graphene-based flexible anodes still faces many challenges.

2.1.4. Carbon Cloth-Based Anodes

Compared with the above mentioned carbon nanofibers, graphene, and carbon nanotubes, carbon cloth is also proposed as a conductive substrate for flexible LIB anode because of its excellent corrosion resistance, outstanding mechanical flexibility and tensile strength, high conductivity, and commercial availability. Growing or coating/depositing high capacity active materials on 3D carbon cloth has been found to be a useful way for constructing the flexible anodes of lithium ion batteries. A number of carbon cloth-based anode materials have been employed to fabricate the flexible LIBs (**Figure 5** and **Table 4**), such as SnO$_2$@Si/carbon cloth,[76] NiO nanosheets/carbon cloth,[77] MoS$_2$ nanoflake array/carbon cloth,[78] titanium dioxide@titanium nitride nanowires/carbon cloth,[79] CoMoO$_4$ nanowire arrays/carbon cloth,[80] FeS@C/carbon cloth,[81] SnO$_2$@TiO$_2$ double-shell nanotubes/carbon cloth,[82] carbon nanotube array/carbon cloth,[83] VO$_2$(B)/carbon cloth,[84] α-Fe$_2$O$_3$ nanorods/carbon cloth,[85] porous CoFe$_2$O$_4$ nanowire arrays/carbon cloth,[86] Fe$_2$O$_3$@carbon/carbon cloth,[87] and MoS$_2$@C/carbon cloth.[88] The outstanding performance of carbon cloth-based anode in LIBs can be attributed to the synergetic effect of high conductive carbon cloth and high capacity active materials.

A new method was proposed for synthesizing SnO$_2$@Si/carbon cloth anode based on the CVD process and subsequent depositing.[76] The SnO$_2$ nanowires grown on the carbon cloth (1.5 cm × 3 cm) serve as both conductive frame and active materials, providing a strong support to deposit a thin layer Si
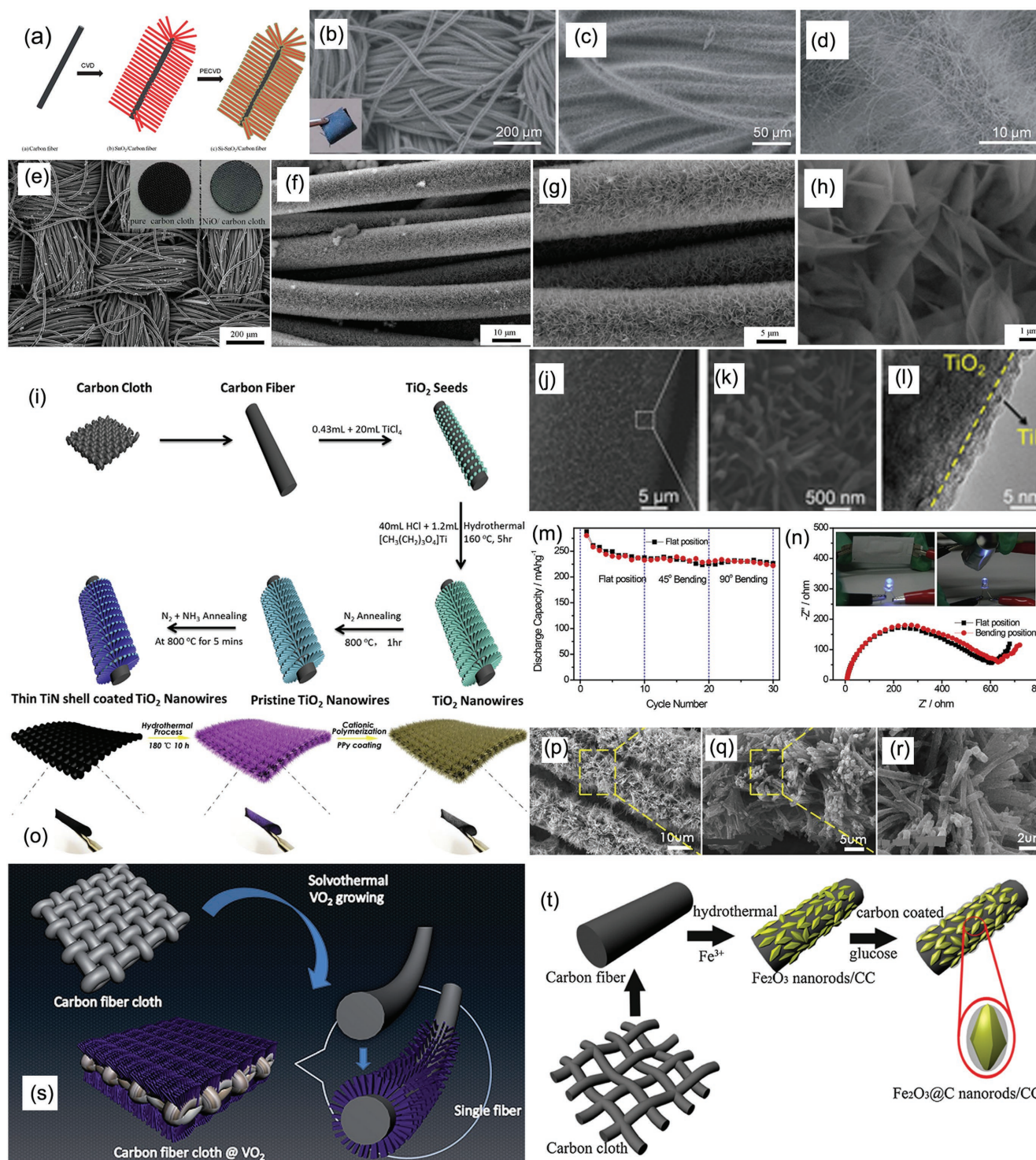
Figure 5. a) Schematic illustration of the growth process and b–d) SEM images of the SnO$_2$@Si core–shell nanowire arrays on carbon cloth. e–h) SEM images of the NiO nanosheets/carbon cloth with well-established textiles at different magnifications. i) Schematic illustration of the synthesis process. j,k) SEM images and l) TEM image of the TiO$_2$@TiN nanowires on carbon cloth, and m) its corresponding cyclic performance. n) Nyquist plot of the device at the normal and bending position. o) Schematic diagram showing the fabrication process of CoMoO$_4$/polypyrrole (PPy) composites grown on carbon cloth. p–r) SEM images CoMoO$_4$/PPy core–shell nanowire arrays on carbon cloth. s) Schematic illustration showing the fabrication process of carbon fiber cloth (CFC)@VO$_2$ composite. t) Schematic illustration displaying the fabrication process of Fe$_2$O$_3$@C nanorods grown on carbon cloth. a–d) Reproduced with permission.[76] Copyright 2013, Royal Society of Chemistry. e–h) Reproduced with permission.[77] Copyright 2014, Nature Publishing Group. i–n) Reproduced with permission.[79] Copyright 2014, Elsevier. o–r) Reproduced with permission.[80] Copyright 2015, Elsevier. s) Reproduced with permission.[84] Copyright 2016, Royal Society of Chemistry. t) Reproduced with permission.[87] Copyright 2016, Elsevier.

Table 4. Carbon cloth based flexible anodes used in LIBs.

Materials	Synthesis process	Test condition	Performance	Ref.
SnO$_2$@Si core–shell nanowire arrays/carbon cloth	CVD + plasma-enhanced CVD	Swagelok-type/0.01–3 V	1.4 mAh cm^{-1}/50 cycles/0.38 mA cm^{-1}	[76]
NiO Nanosheets/carbon cloth	Solution method + annealing	Coin cell/0.01–3 V	892.6 mAh g^{-1}/120 cycles/100 mA g^{-1}	[77]
MoS$_2$ nanoflake array/carbon cloth	One-step hydrothermal synthesis	Coin cell/0.001–3 V	3 mAh cm^{-1}/30 cycles/0.15 mA cm^{-1}	[78]
TiO$_2$@titanium nitride nanowires/carbon cloth	Hydrothermal method and annealing	Coin cell/0.01–3 V	202 mAh g^{-1}/650 cycles/3350 mA g^{-1}	[79]
CoMoO$_4$ nanowire arrays/carbon cloth	Two-step solution based approach	Coin cell/0.01–3 V	764 mAh g^{-1}/1000 cycles/1200 mA g^{-1}	[80]
FeS@C/carbon cloth	Hydrothermal method + carbonization treatment	Coin cell/0.01–3 V	420 mAh g^{-1}/100 cycles/91.35 mA g^{-1}	[81]
SnO$_2$@TiO$_2$ double-shell nanotubes/carbon cloth	Hydrothermal method + atomic layer deposition	Coin cell/0.01–3 V	779 mAh g^{-1}/100 cycles/780 mA g^{-1}	[82]
Vertically aligned carbon nanotube/carbon cloth	Plasma enhanced chemical vapor deposition	Coin cell/0.01–1.2 V	2.51 mAh cm^{-1}/200 cycles/0.2 mA cm^{-1}	[83]
VO$_2$(B)/carbon cloth	One-pot solvothermal method	Coin cell/2–3 V	138 mAh g^{-1}/100 cycles/100 mA g^{-1}	[84]
Porous CoFe$_2$O$_4$ nanowire arrays/carbon cloth	Hydrothermal method + annealing	Coin cell/0.005–3 V	1204 mAh g^{-1}/200cycles/500 mA g^{-1}	[86]

film with high charge capacity. The SnO$_2$@Si/ carbon cloth as a flexible anode for LIBs shows an enhanced electrochemical performance. A cost-effective method composed of a solution treatment and an annealing process was developed to directly grow interconnected mesoporous NiO nanosheets on 3D carbon cloth, which was employed as flexible anode to fabricate flexible LIBs.[77] The as-assembled flexible battery can light a LED glub and several nixie tubes under bending state, respectively. A 3D hierarchical MoS$_2$ nanoflake array/carbon cloth synthesized by one-step hydrothermal method was used as the flexible anode for LIBs.[78] After continuous bending for 50 cycles, the full bendable battery consisting of LiCoO$_2$ cathode and the flexible MoS$_2$ nanoflake array/carbon cloth anode can still offer a power for a commercial red LED light. A TiO$_2$@TiN nanowires/carbon cloth prepared via a hydrothermal method and subsequent annealing was also suggested as anode to build flexible LIBs.[79] The as-assembled LiCoO$_2$//TiO$_2$@TiN/carbon cloth flexible lithium-ion battery lightened a blue LED glub under great bending state.

A two-step solution-based approach was developed to construct a flexible composite anode of 3D CoMoO$_4$/polypyrrole core–shell nanowire arrays on carbon cloth.[80] First, CoMoO$_4$ nanowires were grown on the pretreated carbon cloth substrate in an autoclave at 180 °C for 10 h. Then, the polypyrrole shells as a conductive layer were coated on the outer surface of CoMoO$_4$ nanowires for synthesizing the CoMoO$_4$/polypyrrole core–shell nanowire arrays/carbon cloth composite anode. It was believed that this method could be a reliable technique to prepare the excellent flexible integrated anode materials for LIBs. A hydrothermal approach combined with a carbonization process was used to build a flexible anode of FeS@C/carbon cloth for LIBs.[81] In this hybrid system, the carbon cloth serves as a highly conductive framework to support nanostructured FeS, and the carbon protection layer on FeS surface suppresses the volume change during cycling, resulting in its improved electrochemical performance. A novel hierarchical carbon nanostructure of vertically aligned carbon nanotube array

coated on carbon cloth was employed as a 3D flexible current collector to support growth of thick Si film.[83] The synthesized carbon nanotube array–Si/carbon cloth nanocomposite as a flexible anode for LIBs has distinct advantages including high structural stability and outstanding Li storage property.

2.1.5. Other Materials for Fabricating Flexible Anodes

Similar to the conductive flexible substrates mentioned above such as carbon nanofibers, graphene, carbon cloth, and carbon nanotubes, other 3D carbon based materials including carbon fabric,[89–91] carbon textile,[92–94] expanded graphite paper,[95] and carbon foam[96] have been demonstrated to be promising current collectors to support active materials for building flexible anodes due to their light weight and excellent flexibility (**Figure 6**). For example, a flexible LIB composite anode of TiN nanowires/carbon fabric was constructed by a two-step approach combining a hydrothermal method and annealing,[89] which could deliver a discharge capacity of 455 mAh g^{-1} after 100 cycles at 335 mA g^{-1}. Mesoporous NiCo$_2$O$_4$ nanowire arrays growing on carbon textiles as self-supported anodes for LIBs were built via a surfactant-assisted hydrothermal approach combined with a postannealing process.[92] The fabricated NiCo$_2$O$_4$/carbon textile flexible anodes show a high reversible capacity of 854 mAh g^{-1} after 100 cycles at 0.5 A g^{-1}. Co$_3$O$_4$ nanoparticle-modified expanded graphite paper was synthesized to fabricate flexible, binder-free, and low cost anodes of LIBs,[95] showing a high capacity of 722 mAh g^{-1} after 50 cycles at high current density of 100 mA g^{-1}. New NiCo$_2$S$_4$ nanotube arrays/nitrogen-doped carbon foam composite was also fabricated via a surfactant-assisted hydrothermal approach combined with a sulfurization treatment.[96] The obtained special 3D structure combining the advantages of both active materials and flexible substrate is employed as flexible anodes to improve the electrochemical performances of LIBs (1182 mAh g^{-1} at high current density of 500 mA g^{-1} after 100 cycles).

**ADVANCED
SCIENCE NEWS**

www.advancedsciencenews.com

**ADVANCED
MATERIALS
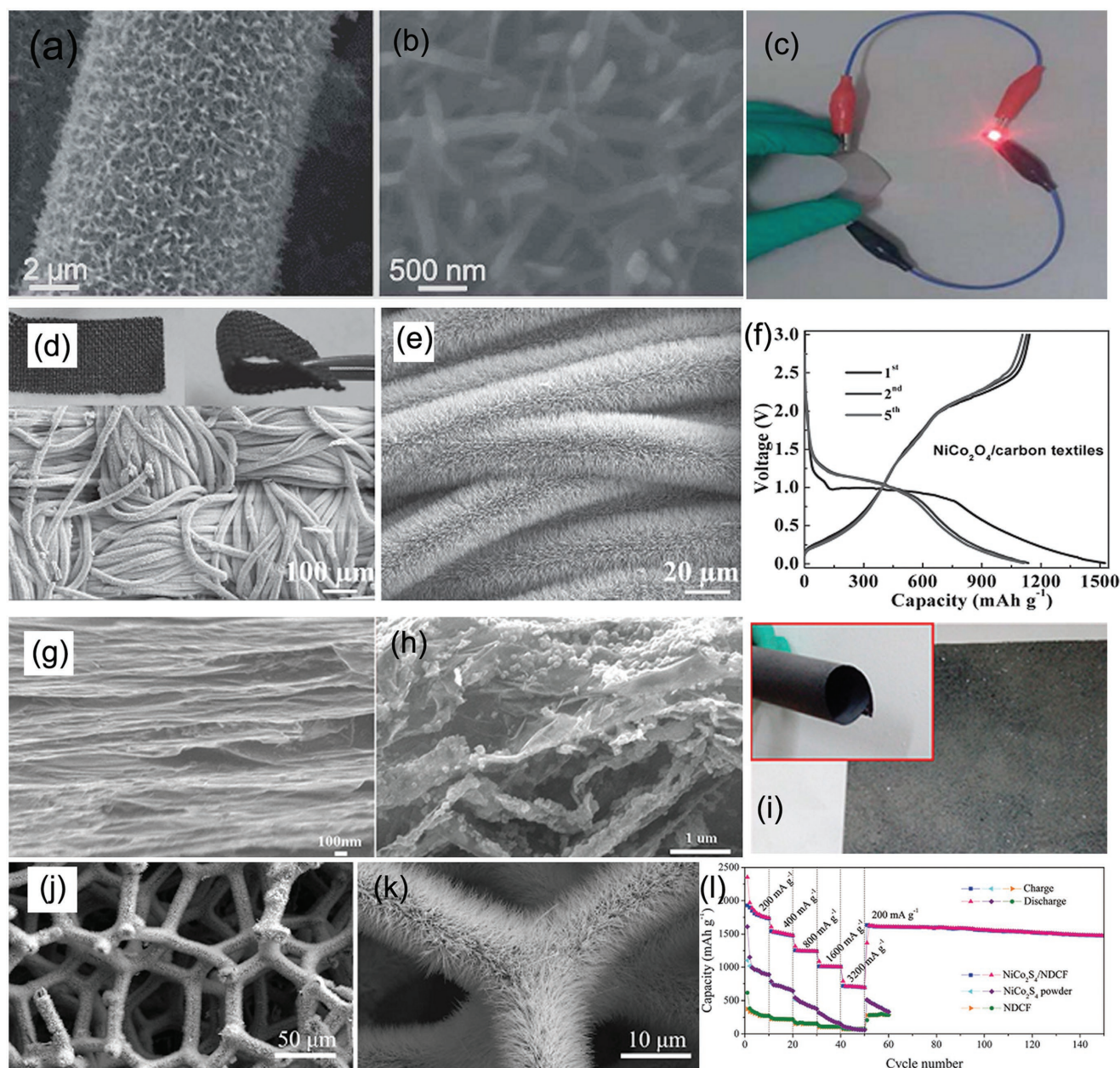TECHNOLOGIES**

www.advmattechnol.de

Figure 6. a,b) SEM images of TiN-900 and c) demonstration of the full battery (LiCoO$_2$//TiN-900) lightening a red LED in the bent position. d,e) Low, high magnification SEM images, and f) charge–discharge voltage profiles of the crystalline NiCo$_2$O$_4$ nanowire arrays (NWAs)/carbon textiles composite. g–i) SEM images and digital image of Co$_3$O$_4$/expanded graphite (EG) paper. j,k) SEM images and l) rate capability of the NiCo$_2$S$_4$/nitrogen-doped carbon foam (NDCF) composites. a–c) Reproduced with permission.[89] Copyright 2014, Royal Society of Chemistry. d–f) Reproduced with permission.[92] g–i) Reproduced with permission.[95] Copyright 2015, Elsevier. j–l) Reproduced with permission.[96] Copyright 2016, Royal Society of Chemistry.

Besides the carbon based materials discussed above, nanostructured active materials are directly employed to construct the flexible anodes of LIBs because of their light weight, high surface area, and good flexibility (**Figure 7**), such as 3D web-like Li$_4$Ti$_5$O$_{12}$ nanostructure[97] and sandwich-type CN$_x$/CuO/CN$_x$ nanocomposite.[98] Although these active materials greatly raise the mass loading of anode materials, the obtained anodes tend to suffer from their low electrical conductivity. Therefore, further enhancing their electrical conductivity and lowering their

production cost are necessary for the future development of nanostructured active materials based anodes.

2.2. Flexible Cathodes

As an important component of LIBs, cathode materials with large capacity and high discharge voltage platform have been studied for two decades and play a key role in the determination
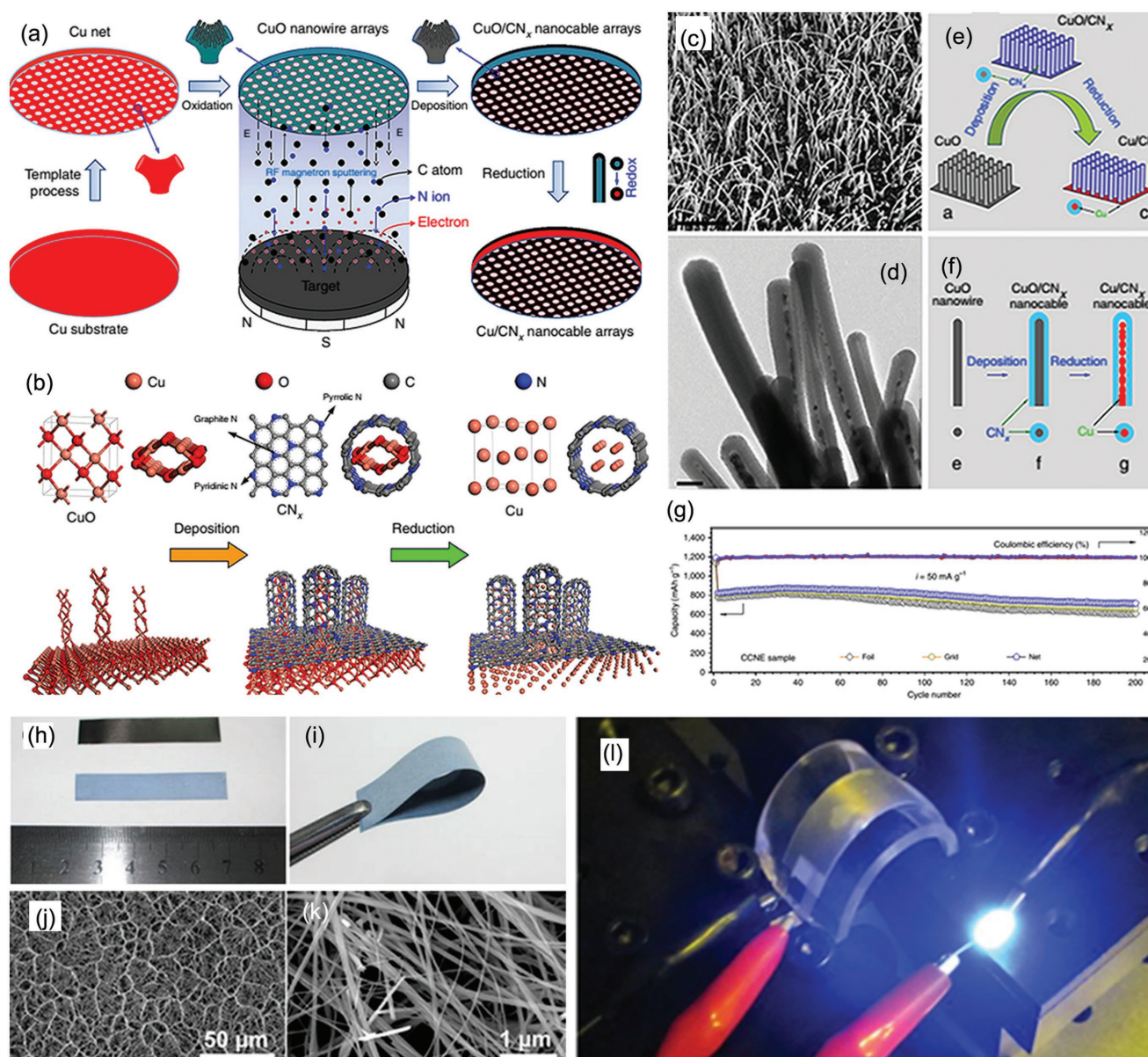
Figure 7. a) Schematic illustration showing the fabrication process of a binder-free 3D array with core–shell nanoarchitecture. b) Theoretical structural modelling displaying the micromechanism of CuO nanowire electrode (CNE), CuO/CNx nanocable electrode (CCNE), and Cu/CNx nanocable electrode (CNNE) formation. c) SEM and d) TEM image of CNNE. e,f) Schematic of the synthesizing processes of the nanosubstrate and g) their rate performance. h,i) Digital photos of the titanium foil before and after the reaction. j,k) SEM images of the web-like LTO nanostructures assembled with nanowires. l) Demonstration of the full battery lighting a blue LED device under bending. a–g) Reproduced with permission.[98] Copyright 2016, Nature Publishing Group. h–l) Reproduced with permission.[97] Copyright 2014, Springer.

of the electrochemical performances of LIBs. A variety of cathodes materials have been studied for LIBs, such as $LiCoO_2$, $LiMn_2O_4$, $LiFePO_4$, and V_xO_y, however their low conductivities lead to a poor rate capability of LIBs. Incorporating these cathode materials with various flexible conducting matrixes, such as carbon based materials (e.g., CNTs,[99–104] graphene,[105,106] carbon nanofibers,[107] ultrathin graphite foam,[108] and carbon cloth[109]), metal materials (e.g., Ti fabric[110]), and organic polymers (e.g., thermoplastic polyurethane[111]), is an effective method for improving the conductivities, stability, and performances of cathodes materials, which have been paid more attention (**Figure 8**).

The direct growth of cathode materials on flexible substrates is a big challenge, because most flexible substrates are not chemically stable at the high temperature (>700 °C) used for synthesizing cathode materials. Therefore, a facile electrodepostion and solvothermal lithiation strategy was proposed to fabricate a $LiMn_2O_4$/CNT paper composite flexible cathode.[112] First, MnO_2/CNT paper composite was built via electrodepostion, and then lithiated to form spinel $LiMn_2O_4$/CNT paper composite by solvothermal lithiation. The synthesized $LiMn_2O_4$/CNT paper flexible cathode still remains above 58.8% of its initial capacity after bending 4000 cycles. A electrospinning

**ADVANCED
SCIENCE NEWS**

www.advancedsciencenews.com

**ADVANCED
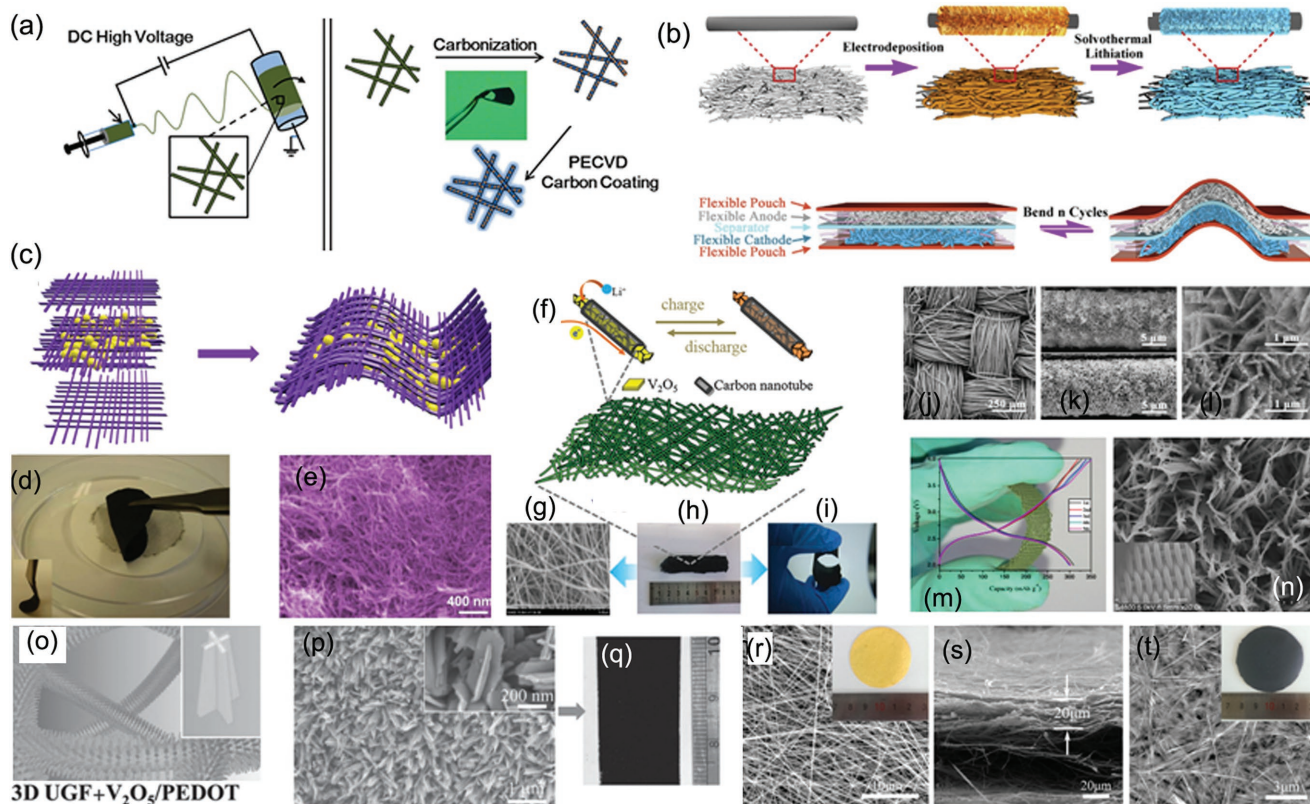MATERIALS
TECHNOLOGIES**

www.advmattechnol.de

Figure 8. a) Schematic illustrations of the electrospinning fabrication of LVP/PAN composite nanofibers and the formation of LVP/CNFs. b) Schematic illustration of the fabrication procedure of flexible batteries with CNT@LiMn$_2$O$_4$ cathodes and graphitized carbon fiber (GCF) anodes. c) Schematic illustration of the fabrication procedure. d) Digital photo and e) SEM image of the LiNi$_{0.5}$Mn$_{1.5}$O$_4$@MWCNT electrodes. f–i) Electrode design and fabrication of self-supported flexible V$_2$O$_5$@G membrane. j–l) SEM images of LiMn$_2$O$_4$ or Mn$_3$O$_4$ nanowall arrays grown on the carbon cloth at different magnifications. m) Digital photo. n) SEM image and charge–discharge voltage profiles of the as-synthesized hierarchical KVO nanowires with an inset of Ti fabric. o) Schematics. p) SEM image. q) Digital photo of ultrathin graphite foam (UGF)–V$_2$O$_5$/polymer poly(3,4-ethylenedioxythiophene) (PEDOT) core/shell nanobelts. r–t) The surface and cross-section SEM images of the pure V$_2$O$_5$ NWs paper (left) and the V$_2$O$_5$/rGO composite paper (right) (inset: digital picture). a) Reproduced with permission.[107] Copyright 2016, Royal Society of Chemistry. b) Reproduced with permission.[112] Copyright 2017, Elsevier. c–e) Reproduced with permission.[100] Copyright 2015, Elsevier. f–i) Reproduced with permission.[102] Copyright 2016, Royal Society of Chemistry. j–l) Reproduced with permission.[109] Copyright 2016, Elsevier. m,n) Reproduced with permission.[110] Copyright 2017, Elsevier. o–q) Reproduced with permission.[108] r–t) Reproduced with permission.[105] Copyright 2017, American Chemical Society.

process combined with a CVD method was developed to synthesize V$_2$O$_5$ nanosheets@CNTs flexible cathode,[102] which shows an excellent Li ion storage performance (a reversible capacity of 211 mAh g^{-1} at a current density of 300 mA g^{-1} after 200 cycles). A binder-free and free-standing cathode material composed of V$_2$O$_5$ nanowires and reduced graphene oxide nanosheets was synthesized via a two-step reduction method,[105] in which the reduced graphene oxide nanosheets have the effect in enhancing the electronic conductivity of V$_2$O$_5$ nanowires. The synthesized V$_2$O$_5$ nanowires@RGO composite paper cathode shows 30.9% capacity decay after 1000 cycles at 0.9 mA cm^{-2}. A novel strategy consisted of electrospinning, annealing, and plasma enhanced CVD was used to prepare a flexible cathode of Li$_3$V$_2$(PO$_4$)$_3$ (LVP)@carbon nanofibers composite.[107] Polyacrylonitrile serves as the carbon precursor to prepare Li$_3$V$_2$(PO$_4$)$_3$/carbon nanofibers during the electrospinning and carbonizing process. A smooth thin layer of carbon is coated on the surface of Li$_3$V$_2$(PO$_4$)$_3$/carbon nanofibers via plasma enhanced CVD under acetylene (C$_2$H$_2$) to improve the conductivity of composites and the structural stability of cathode

during the lithiation/delithiation processes. After 500 cycles, the cathode of Li$_3$V$_2$(PO$_4$)$_3$@carbon nanofiber composite delivers a high capacity of 121 mAh g^{-1} at 665 mA g^{-1}.

Another combination method based on CVD, solvothermal synthesis, and electrodeposition method was exploited to fabricate lightweight, integrated, and flexible LIB cathodes of V$_2$O$_5$ nanobelt array/polymer core/3D graphene foam.[108] Such integrated cathode delivers a specific capacity of 260 mAh g^{-1} at 1.5 A g^{-1} after 1000 cycles. In order to prepare a porous LiMn$_2$O$_4$ nanowall/carbon cloth composite, a new one-step "hydrothermal lithiation" strategy was developed.[109] The porous Mn$_3$O$_4$ nanowall arrays were planted on a carbon cloth substrate via cathodic deposition and lithiated in a 50 mL autoclave at 240 °C for 17 h to synthesize the LiMn$_2$O$_4$ nanowall/carbon cloth composite. When it is used as flexible cathode for LIBs, the LiMn$_2$O$_4$ nanowall/carbon cloth composite exhibits a specific capacity of 126.5 mAh g^{-1} at 148 mA g^{-1} after 200 cycles. A titanium (Ti) fabric was employed as flexible substrate to fabricate a potassium vanadates (KVO) nanowires/Ti fabric cathode.[110] KVO nanowires were deposited on the Ti fabric by

**ADVANCED
SCIENCE NEWS**

www.advancedsciencenews.com

**ADVANCED
MATERIALS
TECHNOLOGIES**

www.advmattechnol.de

a hydrothermal method. The built flexible KVO nanowires/Ti fabric cathode shows an improved Li-ion storage performance (270 mAh g^{-1} at 100 mA g^{-1} after 300 cycles). Also, a polymer material, polyurethane, was proposed as a free-standing matrix to synthesize a flexible LiFePO$_4$-based cathode.[111] The conductive carbon and LiFePO$_4$ particles are uniformly dispersed in the porous flexible polyurethane matrix using a phase separation method. The obtained LiFePO$_4$/super P/polyurethane composites as flexible cathode for LIBs can remain 98.6% of its initial capacity after 100 cycles at 170 mA g^{-1}.

Although significant efforts to develop the flexible inorganic cathodes of LIBs have been made, inorganic cathode materials are brittle and have a poor elastic deformation limit. Therefore, some polymer active materials with high theoretical capacity, high conductivity, and inherent flexibility are proposed as organic cathode materials for high-performance flexible LIBs, such as polymerized polyimide,[113] polyimide derivative pyromellitic dianhydride-tris(2-aminoethyl)amine,[104] and organic carbonyl compounds (**Figure 9**).[114] An organic cathode based on the polyimide vertically grew on a SWCNT film was synthesized by in situ polymerization,[113] in which the SWCNT film serves

as a lightweight current collector for improving the electronic conductivity of cathodes. The synthesized flexible polyimide@SWCNT film shows an excellent mechanical property and electrochemical performance (175 mAh g^{-1} at a current density of 221.5 mA g^{-1} after 200 cycles). Another organic flexible cathode with a nanocable structure consisted of polyimide derivative pyromellitic dianhydride-tris(2-aminoethyl)amine (PMTA) and SWCNT was fabricated by a simple rolling process.[104] The network of carbon nanotubes coated on the nanocable composites of SWCNT/PMTA can enhance the electronic conductivity of cathodes. The obtained SWCNT/PMTA/SWCNT flexible cathode can remain 86.6% of its initial capacity (147 mAh g^{-1}) at 191.5 mA g^{-1} over 200 cycles. Furthermore, sodium 1,4-dioxonaphthalene-2-sulfonate (NQS) is one kind of organic carbonyl compound. NQS can not effectively hinder the dissolution of organic carbonyl compounds in electrolyte, but also has a high reduction potential, when it is used as cathode active materials for LIBs.[114] The introduction of multiwalled carbon nanotubes (MWNTs) into NQS for preparing the flexible cathode of NQS/MWNTs can improve the electronic conductivity of electrode. The binder-free, flexible, and free-standing composite
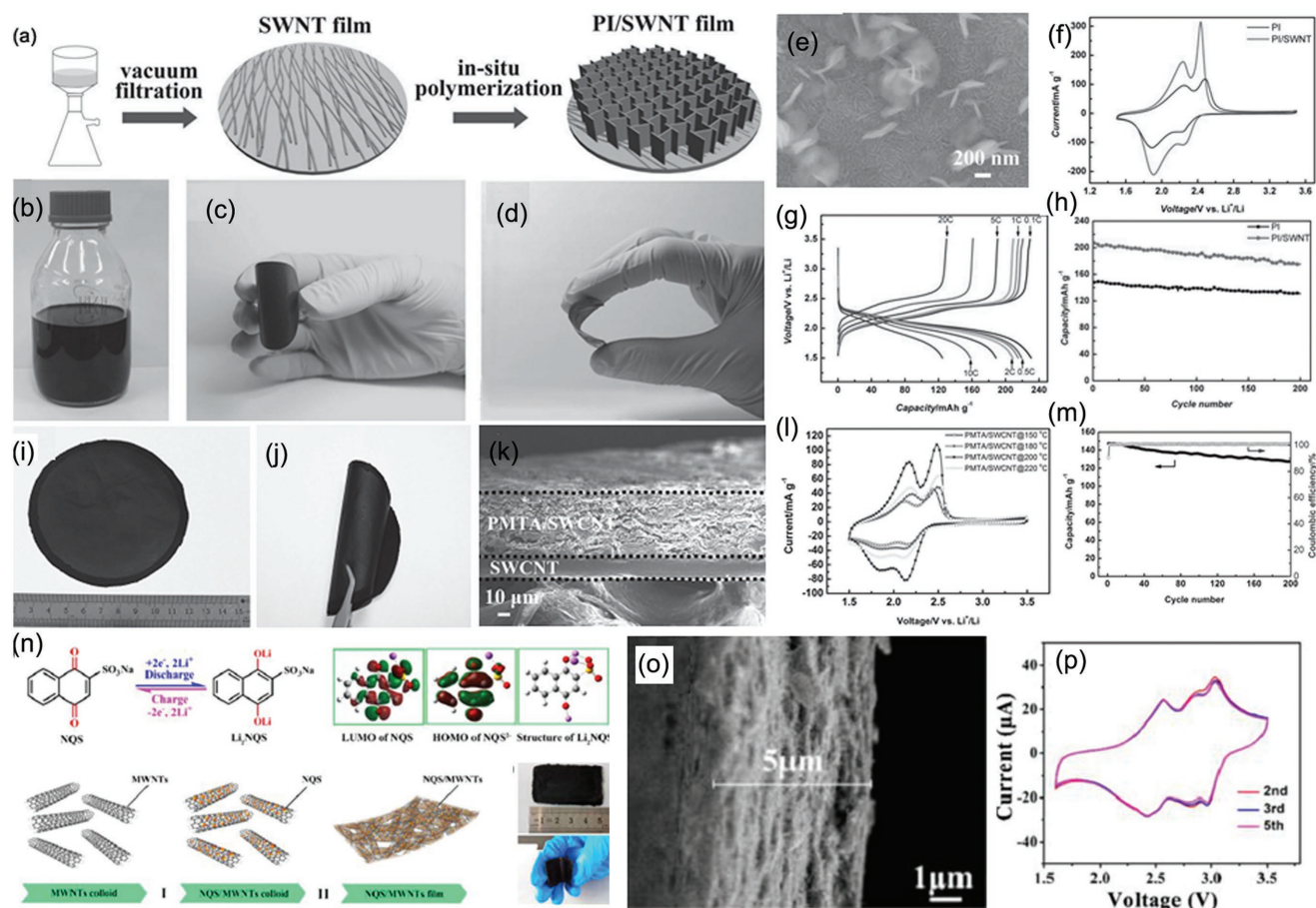

Figure 9. a) Schematic of the fabrication process of polyimide (PI)/single-wall carbon nanotube (SWNT) film. b–d) Digital photos of SWNT aqueous dispersion, SWNT film, and PI/SWNT film. e) SEM. f) Cyclic voltammetry. g) Galvanostatic charging/discharging curves. h) Cycling performance of PI/SWNT film. i,j) Photographs, k) cross-sectional SEM images, l) cyclic voltammetry, and m) cycling performance of the flexible PMTA/SWCNT@SWCNT electrode. n) Schematic process for synthesizing NQS/MWNTs hybrid films and their photographs (inset). o) Cross-sectional SEM image. p) CV profiles of NQS/MWNTs of a NQS/MWNTs hybrid film. a–h) Reproduced with permission.[113] i–m) Reproduced with permission.[104] n–p) Reproduced with permission.[114] Copyright 2017, American Chemical Society.

**ADVANCED
SCIENCE NEWS**
www.advancedsciencenews.com

**ADVANCED
MATERIALS
TECHNOLOGIES**
www.advmattechnol.de

cathode of NQS/MWNTs synthesized by a facile dissolution–recrystallization method maintains 96% of its initial capacity (155 mAh g^{-1}) at 41.2 mA g^{-1} over 50 cycles.

In general, cathode materials including inorganic active materials and organic active materials for LIBs possess high capacity but usually suffer from bad conductivity. Conducting flexible substrates have poor capacity but high conductivity. It has been demonstrated that incorporating cathode active materials in flexible substrates is a good approach to build desirable flexible LIB cathodes. However, the relatively low yield and high cost are the two bigger challenges in the realization and application of flexible LIB cathodes.

3. Flexible Electrolytes

Liquid electrolyte with a high ionic conductivity is an important component for building a commercial Li-ion battery. However, its disadvantages including flammability, toxicity, volatility, fluidity, and a potential danger of leakage greatly limit the application of liquid electrolyte in a flexible battery. Therefore, more efforts have been paid to develop polymer based electrolytes

to replace liquid ones.[7] Polymer electrolytes with an inherent flexibility, a wide electrochemical window, low toxicity, and high safety, such as polymer gel electrolytes and solid-state polymer electrodes, have been employed in the design and fabrication of flexible LIBs.

Among various polymer electrolytes, gel polymer electrolytes (GPEs), composed of conventional liquid electrolytes and a polymer matrix, have been extensively investigated because of their good ionic conductivity, nonflammability, high thermal stability, excellent electrolyte leakage-proof ability, and mechanical flexibility (**Figure 10**).[115–122] For example, a self-supporting composite gel polymer electrolyte, consisting of a liquid electrolyte (1 M LiPF$_6$ in ethylene carbonate (EC)/propylene carbonate = 1/1 (v/v)), a UV (ultraviolet)-cured ethoxylated trimethylolpropane triacrylate (ETPTA) mechanical matrix, and Al$_2$O$_3$ nanoparticles (a weight-based composition ratio of the (ETPTA/liquid electrolyte = 15/85 w/w)/Al$_2$O$_3$ = 34/66 w/w), was used in a flexible lithium ion battery, which can conform to 3D micropatterned architecture electrodes.[115] A functional filler of Al$_2$O$_3$ nanoparticles incorporated in the composite gel polymer electrolyte can adjust its rheological properties for direct printing complex-structured electrodes. A cell using the flat composite gel polymer electrolyte shows a
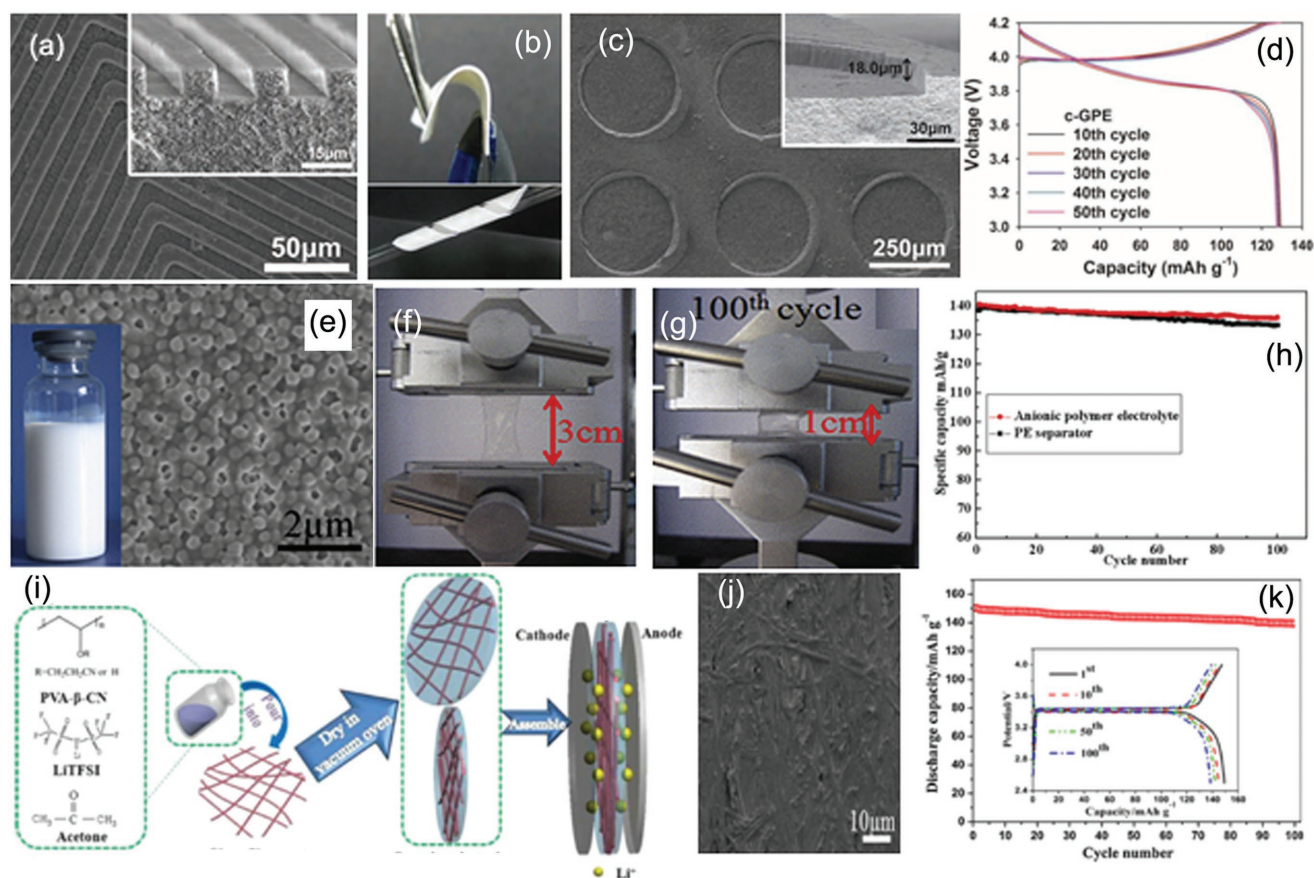

Figure 10. a) A SEM image (surface) (an inset is a cross-sectional image) and b) photographs of a c-GPE with a maze-pattern. c) An SEM image of inversely replicated c-GPE (an inset is a cross-sectional image). d) Charge/discharge profiles of a cell (lithium metal/flat-shaped c-GPE/LiCoO$_2$ cathode). e) SEM photographs. f,g) Mechanical bending test. h) Voltage drop of anionic polymer membrane. i) A schematic illustration showing a rigid-flexible coupling glass-microfiber polymer electrolyte membrane (GFMPE) fabrication process and the corresponding sandwich structure of a coin cell. j) SEM image of GFMPE membrane. k) Cycle performance of LiCoO$_2$/GFMPE-LiN(SO$_2$CF$_3$)$_2$ (LS)/graphite cells. a–d) Reproduced with permission.[115] e–h) Reproduced with permission.[118] Copyright 2014, Elsevier. i–k) Reproduced with permission.[119] Copyright 2015, Elsevier.

**ADVANCED
SCIENCE NEWS**
www.advancedsciencenews.com

**ADVANCED
MATERIALS
TECHNOLOGIES**
www.advmattechnol.de

good cycling performance (about 125 mAh g^{-1} after 50 cycles) between 3.0 and 4.2 V. An anionic polymer electrolyte was synthesized by soaking an anionic polymer membrane (a mass ratio of methyl acrylate:acrylonitrile:ammonium persulfate = 9:1:0.25) in an electrolyte solution (1 M LiPF$_6$ in ethylene carbonate (EC)/dimethyl carbonate (DMC)/diethyl carbonate(DEC) (1:1:1 in volume)).[118] The anionic polymer electrolyte with good mechanical flexibility employed in a flexible lithium ion battery exhibited an improved cycling performance (135 mAh g^{-1} after 100 cycles). Triethylene glycol diacetate-2-propenoic acid butyl ester (TEGDA-BA) based composite polymer electrolytes with 5 wt% Al$_2$O$_3$ nanoparticles were prepared by heating a mixture (Al$_2$O$_3$, TEGDA, BA, C$_{14}$H$_{24}$N$_4$, and 1 M LiPF$_6$ in EC/DMC/DEC (1:1:1 in volume), liquid electrolytes/comonomer = 94/6 w/w) at 80 °C for 30 min via in situ thermal polymerization.[117] The obtained composite polymer electrolytes with high ionic conductivity (6.02 × 10^{-3} S cm^{-1} at 25 °C) for use in flexible lithium ion batteries show a stable charge/discharge performance (160 mAh g^{-1} after 200 cycles).

Using solid-state electrolytes leads to the improved safety, flexibility, and shape-compatibility of the LIBs; however, their lower conductivity decreases the rate performance of batteries. Therefore, exploring new solid-state electrolytes with high ionic/electronic conductivity is important for high-performance

flexible LIBs. Furthermore, enhancing the stability of interface between the solid-state electrolytes and electrodes, advancing the mechanical strength and the structural integrity of solid-state electrolytes, and studying the principle design of flexible cells should be paid close attention in the fabrication of flexible LIBs.

4. Full Flexible Cells

To improve practical application of flexible LIBs, continuous efforts should be invested in fabricating full flexible batteries. Effective construction strategies play a critical role in determining the distinguishing features, compatibility, stability, integrity, output, and cost of the flexible LIBs. In the current research, various strategies have been explored to fabricate the flexible LIBs, such as lamination,[123] vacuum filtration,[124] coating,[125] winding,[126] and printing.[127] Although these strategies are suitable for the manufacture of the flexible LIBs in lab scale, most of them cannot be applied in large scale industrial production. Therefore, it should take great effort to search key technologies to increase production yield and reduce the cost of future full cell production.[128–131] To better understand the fabrication process of full flexible, some recent typical examples are listed below (**Figure 11**).
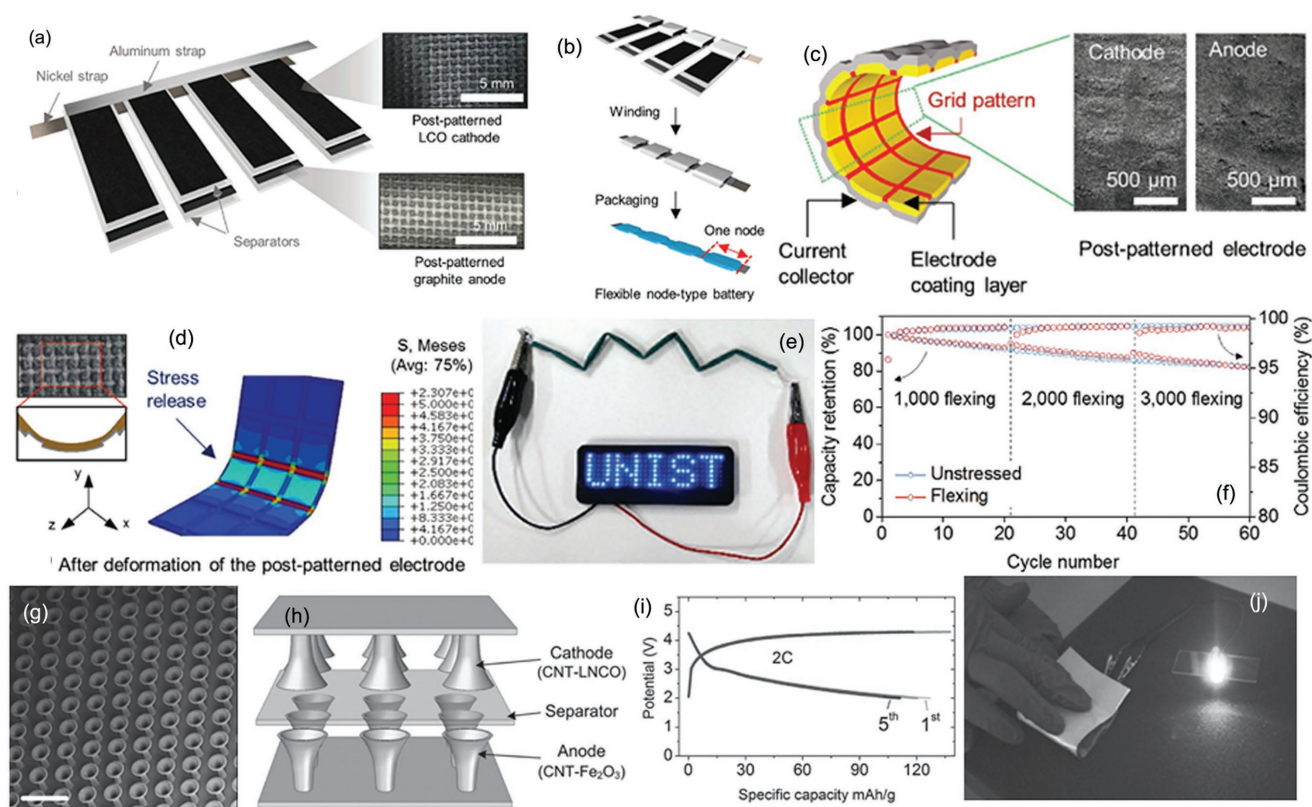

Figure 11. a) A schematic illustration of node-type cell consisting of postpatterned LiCoO$_2$ and graphite electrodes and the corresponding cell assembly process. b) A schematic of the deformed postpatterned electrodes and c) their SEM images after 200 cycles. d) Finite element analysis (FEA) results showing the deformation and von Mises stress distribution. e) The node-type LIBs powering a blue LED panel in a zig-zag state. f) A discharge capacity retention of node-type cell in unstressed and flexing conditions. g) SEM image of transferred CNT-cone-structure assemblies. h) Schematic representation. i) Charge/discharge curves of full cell flexible CNT cone battery. j) Full cell flexible CNT cone battery lighting a 3 V white-light LED. a–f) Reproduced with permission.[126] g–j) Reproduced with permission.[46]

A node-type full flexible LIB cell was fabricated via winding the postpatterned anode and cathode on metal straps.[126] The postpatterned LiCoO$_2$ cathode (a loading density of 13.3 mg cm^{-2}) and graphite anode (a loading density of 5.5 mg cm^{-2}) are synthesized by a conventional slurry (active materials/a conductive agent/poly(vinylidene fluoride) in N-methyl-2-pyrrolidinone solution) coating and pressing process. The foils (Al and Cu) were patterned by the square shape template of nickel mesh with flat wires obtained by a roll-pressing machine. The prepared postpatterned electrodes with high adhesion can secure the structural integrity of the node-type full flexible LIBs during cycling. Furthermore, the node-type cell exhibits a stable cycle performance for 100 cycles. Also, active materials (commercial LiCoO$_2$ powder and Fe$_2$O$_3$ nanoparticles) were incorporated into 3D CNT cone current collector via a drop-casting process for fabricating a full flexible LIB.[46] A polypropylene layer or Whatman borosilicate paper was used as a separator, and 1 M LiPF$_6$ used as electrolyte. The one current collector was prepared by contact printing process.

First, the CNT cones were obtained by elastocapillary aggregation from CNT cylinders, and then transferred to a flexible conductive film (polyvinylidene fluoride (PVDF)/MWNTs/phenyl-C61-butyric acid methyl ester in a ratio of 90:5:5) by contact printing to form the current collector. The 3D CNT cone based flexible batteries achieve a high capacity retention (>70% after 500 cycles) and excellent mechanical properties (bending radius ≈300 µm).

To realize the application of wearable electronics, one of the most important considerations is the construction of sustainable fiber-shaped flexible LIBs with high energy density and good mechanical and environmental stability (**Figure 12**a–j). A coaxial, fibre-shaped full LIB with good performance was fabricated from an aligned CNT/Si hybrid yarn (anode) and an aligned CNT/LiMn$_2$O$_4$ hybrid yarn (cathode) via a winding method.[132] The prepared fiber-shaped full LIB achieves a high linear capacity density (0.22 mAh cm^{-1}) or a high linear energy density (0.75 mWh cm^{-1}). The resulting wearable energy storage textile exhibits an areal energy density of 4.5 mWh cm^{-2}.
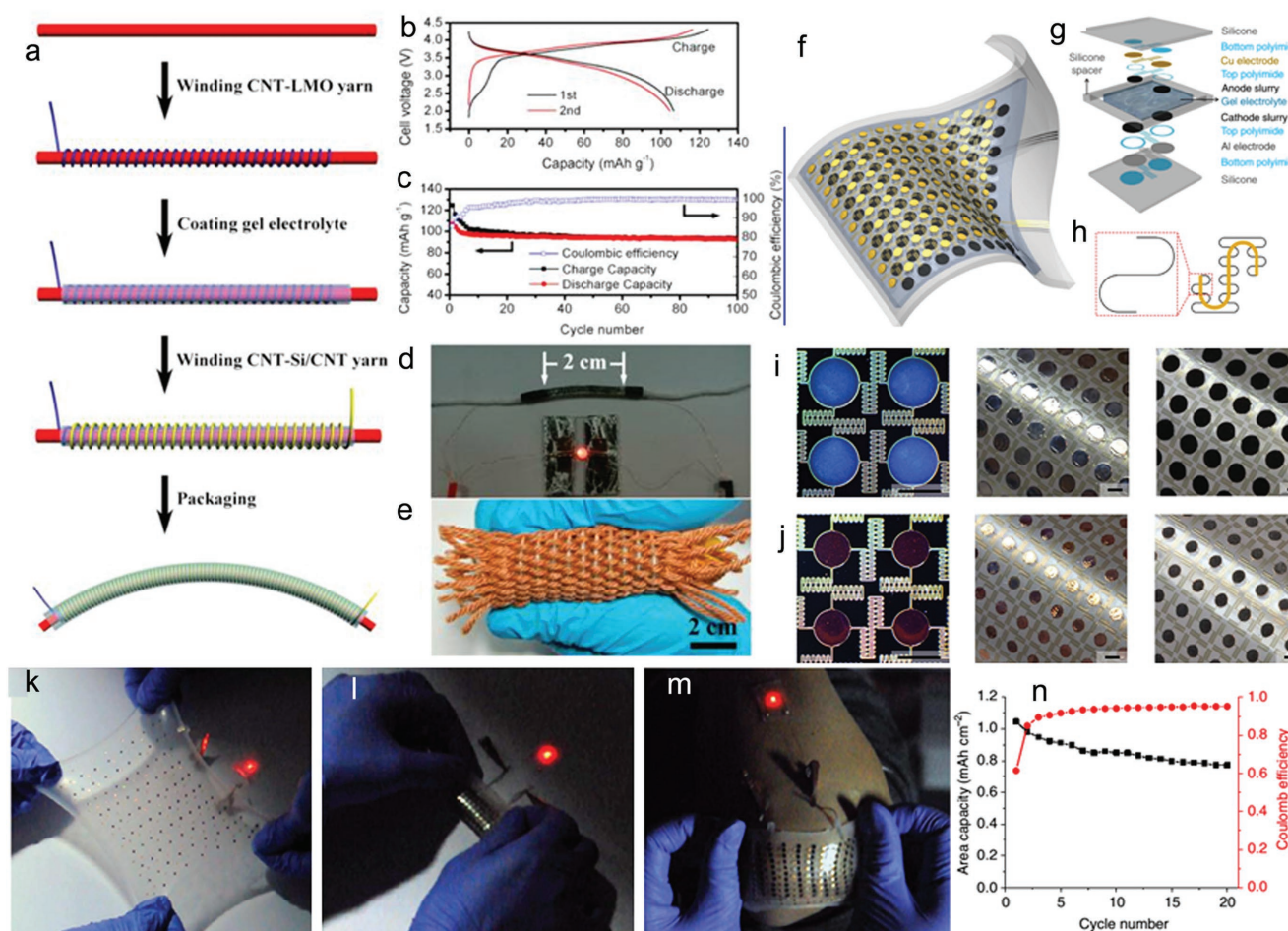

Figure 12. a) Schematic of the fabrication process based on the coaxial fiber full LIB. b) Voltage profiles and c) long-life performance of the fiber-shaped LIB. d) Photograph of the fiber-shaped LIB to power a light emission diode. e) The fiber-shaped full LIBs being woven into a textile. f) Schematic illustration of a completed stretchable device. g) Exploded view layout of the various layers in the battery structure. h) Illustration of "self-similar" serpentine geometries used for the interconnects. Optical images of i) the Al electrode pads and self-similar interconnects on a Si wafer and j) the Cu electrode pads and self-similar interconnects on a Si wafer. Operation of a battery connected to a red light-emitting diodes (LED) while k) biaxially stretched to 300%, l) folded, and m) mounted on the human elbow. n) Capacity retention (black) and coulombic efficiency (red) of the stretchable device over 20 cycles. a–e) Reproduced with permission.[132] Copyright 2014, American Chemical Society. f–n) Reproduced with permission.[133] Copyright 2013, Nature Publishing Group.

**ADVANCED
SCIENCE NEWS**
www.advancedsciencenews.com

**ADVANCED
MATERIALS
TECHNOLOGIES**
www.advmattechnol.de

A full graphite/LiFePO$_4$ paper based LIB cell was produced by a sequential vacuum filtration of water dispersions (sometimes called an aqueous paper-making process).[124] A nanofibrillated cellulose acts as both separator and electrode binder in this system. The paper-battery cells with good flexibility exhibit an energy density of 188 mWh g^{-1} at a current density of 18 mA g^{-1}. A stretchable LIB cell was also fabricated by a strain management technique (Figure 12k–n).[133] The battery is composed of segmented LiCoO$_2$ cathode layers and Li$_4$Ti$_5$O$_{12}$ layers, and they are separated by a gel electrolyte made from a mixture of 10 g polyethylene oxide (4×10^{-6} g mol^{-1}), 100 g lithium perchlorate, 500 mL dimethylcarbonate, and 500 mL ethylene carbonate. Silicone elastomers are employed as stretchable substrates, acryloxy perfluoropolyether elastomer as stretchable encapsulation materials, and a transfer printing technique is used to deposit the active materials on the segmented current collector. The resulting stretchable LIBs can maintain a stable capacity density of about 1.1 mAh cm^{-2} at a potential of 2.35 V, and power light-emitting diodes at a stretching status (>300%).

As discussed above, significant progress has been made on the design and fabrication of full flexible LIBs in the past two years, and their potential application in flexible electronic devices looks extremely promising. However, there are many problems to be resolved in the practical application of full flexible LIBs. Future study on the development of flexible LIBs should focus more on optimizing the cell components (i.e., the electrolytes, electrodes, current collectors, and packaging materials) in terms of their structure characteristics, and exploring new construction technology to improve their safety performance, mechanical stability, and electrochemical performance.

5. Conclusions and Perspectives

The recent advances in flexible LIBs have been reviewed briefly, with special emphasis on the electrode materials, flexible current collectors, flexible solid-state electrolytes, and the structural design and construction of full flexible battery cells. Different electrodes, electrolytes, and related synthesis methods have their own merits and disadvantages.

An ideal flexible battery cell should have these basic features: light weight, low cost, high performance, good structural stability, high safety, and scalable production. To achieve this, more viable electrode, electrolyte, and packaging materials should be investigated and the advanced cell assembly technology needs to be developed. The advances in exploring both high performance flexible anode and cathode materials can offer an excellent platform for developing practical flexible power sources. Synthesizing the composite or hybrid electrodes that combine their advantages to each other due to synergistic effects is a good approach to achieve high performance in flexible LIBs. Some features of solid-state electrolytes, including the flexibility, safety, and conductivity, greatly affect the compatibility and integrity of final cells. Optimizing the electrolyte and electrode interface can enhance the cell safety and utilization ratio of the active materials surface.

In spite of great achievements about the above mentioned flexible LIBs, many challenges still remain for future research. Improving their energy density and power density is important

for the development of full flexible LIBs. Safety is also very critical for their practical applications. Further study regarding the flexible LIBs should focus on the fabrication technologies and mechanical properties of devices, not only on the materials. The performance evaluation standards of the full flexible LIBs should be made, and the mechanical properties, compatibility, and ionic conductivity of solid state electrolytes should be enhanced. Innovating cell structural design and assembly and selecting suitable packaging materials need also to be given more attention. Manufacturing equipments for the industrialization of flexible LIBs should be explored. Modern flexible electronic devices not only depend on flexible LIBs, but need multifunctional devices.

Developing various flexible LIBs including cable/wire type for practical applications such as miniaturized electronic devices is an important research direction in the future. Along with the technical unceasing progress, it is believed that novel flexible LIBs can result in many advances in fabricating technology of flexible electronic devices such as smart electronics, wearable devices, and roll-up displays. Furthermore, the other flexible energy storage and conversion systems including the flexible Li–O$_2$ battery as a promising candidate for the next-generation flexible electrochemical energy storage devices should be considered.[134–138]

[1] W. Liu, M. S. Song, B. Kong, Y. Cui, *Adv. Mater.* **2017**, *29*, 1603436.
[2] L. Li, Z. Wu, S. Yuan, X. B. Zhang, *Energy Environ. Sci.* **2014**, *7*, 2101.
[3] C. Y. Wang, G. G. Wallace, *Electrochim. Acta* **2015**, *175*, 87.
[4] L. Noerochim, J. Z. Wang, D. Wexler, M. Rahman, J. Chen, H. K. Liu, *J. Mater. Chem.* **2012**, *22*, 11159.
[5] Y. H. Hu, X. L. Sun, *J. Mater. Chem. A* **2014**, *2*, 10712.
[6] S. Y. Lee, K. H. Choi, W. S. Choi, Y. H. Kwon, H. R. Jung, H. C. Shin, J. Y. Kim, *Energy Environ. Sci.* **2013**, *6*, 2414.
[7] G. M. Zhou, F. Li, H. M. Cheng, *Energy Environ. Sci.* **2014**, *7*, 1307.
[8] H. Gwon, J. Hong, H. Kim, D. H. Seo, S. Jeon, K. Kang, *Energy Environ. Sci.* **2014**, *7*, 538.
[9] L. Wen, F. Li, H. M. Cheng, *Adv. Mater.* **2016**, *28*, 4306.
[10] M. S. Balogun, W. T. Qiu, Y. Luo, H. Meng, W. J. Mai, A. Onasanya, T. K. Olaniyi, Y. X. Tong, *Nano Res.* **2016**, *9*, 2823.
[11] Y. X. Wang, B. Liu, Q. Y. Li, S. Cartmell, S. Ferrara, Z. Q. D. Deng, J. Xiao, *J. Power Sources* **2015**, *286*, 330.

[12] W. H. Li, M. S. Li, M. Wang, L. C. Zeng, Y. Yu, *Nano Energy* **2015**, *13*, 693.

[13] W. H. Li, Z. Z. Yang, Y. Jiang, Z. R. Yu, L. Gu, Y. Yu, *Carbon* **2014**, *78*, 455.

[14] M. Zhang, F. L. Yan, X. Tang, Q. H. Li, T. H. Wang, G. Z. Cao, *J. Mater. Chem. A* **2014**, *2*, 5890.

[15] W. H. Li, Z. Z. Yang, J. X. Cheng, X. W. Zhong, L. Gu, Y. Yu, *Nanoscale* **2014**, *6*, 4532.

[16] W. H. Li, M. S. Li, Z. Z. Yang, J. Xu, X. W. Zhong, J. Q. Wang, L. C. Zeng, X. W. Liu, Y. Jiang, X. Wei, L. Gu, Y. Yu, *Small* **2015**, *11*, 2762.

[17] C. Wang, W. Wan, Y. H. Huang, J. T. Chen, H. H. Zhou, X. X. Zhang, *Nanoscale* **2014**, *6*, 5351.

[18] C. Y. Zhao, J. H. Kong, X. Y. Yao, X. S. Tang, Y. L. Dong, S. L. Phua, X. H. Lu, *ACS Appl. Mater. Interfaces* **2014**, *6*, 6392.

[19] Y. E. Miao, Y. P. Huang, L. S. Zhang, W. Fan, F. L. Lai, T. X. Liu, *Nanoscale* **2015**, *7*, 11093.

[20] J. Lee, C. S. Jo, B. Park, W. Hwang, H. I. Lee, S. H. Yoon, J. W. Lee, *Nanoscale* **2014**, *6*, 10147.

[21] X. Zhao, Y. X. Du, L. Jin, Y. Yang, S. L. Wu, W. H. Li, Y. Yu, Y. W. Zhu, Q. H. Zhang, *Sci. Rep.* **2015**, *5*, 14146.

[22] T. Wang, H. G. Li, S. J. Shi, T. Liu, G. Yang, Y. M. Chao, F. Yin, *Small* **2017**, *13*, 1604182.

[23] E. Samuel, H. S. Jo, B. Joshi, S. An, H. G. Park, Y. I. Kim, W. Y. Yoon, S. S. Yoon, *Electrochim. Acta* **2017**, *231*, 582.

[24] F. L. Yan, X. Tang, Y. H. Wei, L. B. Chen, G. Z. Cao, M. Zhang, T. H. Wang, *J. Mater. Chem. A* **2015**, *3*, 12672.

[25] J. Wang, W. L. Song, Z. Y. Wang, L. Z. Fan, Y. F. Zhang, *Electrochim. Acta* **2015**, *153*, 468.

[26] L. Xia, S. Q. Wang, G. X. Liu, L. X. Ding, D. D. Li, H. H. Wang, S. Z. Qiao, *Small* **2016**, *12*, 853.

[27] Y. X. Wang, X. F. Wen, J. Chen, S. N. Wang, *J. Power Sources* **2015**, *281*, 285.

[28] M. Dirican, O. Yildiz, Y. Lu, X. M. Fang, H. Jiang, H. Kizil, X. W. Zhang, *Electrochim. Acta* **2015**, *169*, 52.

[29] Y. Z. Wan, Z. W. Yang, G. Y. Xiong, R. S. Guo, Z. Liu, H. L. Luo, *J. Power Sources* **2015**, *294*, 414.

[30] R. Z. Chen, Y. Hu, Z. Shen, Y. L. Chen, X. He, X. W. Zhang, Y. Zhang, *ACS Appl. Mater. Interfaces* **2016**, *8*, 2591.

[31] L. S. Zhang, Y. P. Huang, Y. F. Zhang, H. H. Gu, W. Fan, T. X. Liu, *Adv. Mater. Interfaces* **2016**, *3*, 1500467.

[32] B. N. Joshi, S. An, H. S. Jo, K. Y. Song, H. G. Park, S. Hwang, S. S. Al-Deyab, W. Y. Yoon, S. S. Yoon, *ACS Appl. Mater. Interfaces* **2016**, *8*, 9446.

[33] V. A. Agubra, L. Zuniga, D. Flores, H. Campos, J. Villarreal, M. Alcoutlabi, *Electrochim. Acta* **2017**, *224*, 608.

[34] B. N. Joshi, S. An, Y. I. Kim, E. P. Samuel, K. Y. Song, I. W. Seong, S. S. Al-Dey, M. T. Swihart, W. Y. Yoon, S. S. Yoon, *J. Alloys Compd.* **2017**, *700*, 259.

[35] H. Q. Li, H. J. Ye, Z. Xu, C. Y. Wang, J. Yin, H. Zhu, *Phys. Chem. Chem. Phys.* **2017**, *19*, 2908.

[36] H. R. Lu, J. Hagberg, G. Lindbergh, A. Cornell, *Nano Energy* **2017**, *39*, 140.

[37] M. L. Mao, F. L. Yan, C. Y. Cui, J. M. Ma, M. Zhang, T. H. Wang, C. S. Wang, *Nano Lett.* **2017**, *17*, 3830.

[38] Y. Z. Wan, Z. W. Yang, G. Y. Xiong, H. L. Luo, *J. Mater. Chem. A* **2015**, *3*, 15386.

[39] M. Dirican, O. Yildiz, Y. Lu, X. M. Fang, H. Jiang, H. Kizil, X. W. Zhang, *Electrochim. Acta* **2015**, *169*, 52.

[40] Y. Huang, Z. X. Lin, M. B. Zheng, T. H. Wang, J. Z. Yang, F. S. Yuan, X. Y. Lu, L. Liu, D. P. Sun, *J. Power Sources* **2016**, *307*, 649.

[41] R. Z. Chen, Y. Hu, Z. Shen, P. Pan, X. He, K. S. Wu, X. W. Zhang, Z. L. Cheng, *J. Mater. Chem. A* **2017**, *5*, 12914.

[42] A. Abnavi, M. S. Faramarzi, A. Abdollahi, R. Ramzani, S. Ghasemi, Z. Sanaee, *Nanotechnology* **2017**, *28*, 255404.

[43] Z. Y. Pan, J. Ren, G. Z. Guan, X. Fang, B. J. Wang, *Adv. Energy Mater.* **2016**, *6*, 1600271.

[44] T. Xiang, S. Tao, W. Y. Xu, Q. Fang, C. Q. Wu, D. B. Liu, Y. Zhou, A. Khalil, Z. Muhammad, W. S. Chu, Z. H. Wang, H. F. Xiang, Q. Liu, L. Song, *ACS Nano* **2017**, *11*, 6483.

[45] Y. H. Cheng, G. Chen, H. B. Wu, M. F. Zhu, Y. F. Lu, *J. Mater. Chem. A* **2017**, *5*, 13944.

[46] S. Ahmad, D. Copic, C. George, M. D. Volder, *Adv. Mater.* **2016**, *28*, 6705.

[47] M. C. Zou, Z. M. Ma, Q. F. Wang, Y. B. Yang, S. T. Wu, L. Yang, S. Hu, W. J. Xu, P. C. Han, R. Q. Zou, A. Y. Cao, *J. Mater. Chem. A* **2016**, *4*, 7398.

[48] Z. M. Ma, Y. S. Wang, Y. B. Yang, M. Yousaf, M. C. Zou, A. Y. Cao, R. P. S. Han, *RSC Adv.* **2016**, *6*, 30098.

[49] C. Kang, E. Cha, R. Baskaran, W. Choi, *Nanotechnology* **2016**, *27*, 105402.

[50] X. X. Li, J. J. Fu, Z. G. Pan, J. J. Su, J. W. Xu, B. Gao, X. Peng, L. Wang, X. M. Zhang, P. K. Chu, *J. Power Sources* **2016**, *331*, 58.

[51] L. Sun, W. B. Kong, H. C. Wu, Y. Wu, D. T. Wang, F. Zhao, K. L. Jiang, Q. Q. Li, J. P. Wang, S. S. Fan, *Nanoscale* **2016**, *8*, 617.

[52] S. M. Cao, X. Feng, Y. Y. Song, H. J. Liu, M. Miao, J. H. Fang, L. Y. Shi, *ACS Appl. Mater. Interfaces* **2016**, *8*, 1073.

[53] T. Xiang, S. Tao, W. Y. Xu, Q. Fang, C. Q. Wu, D. B. Liu, Y. Zhou, A. Khalil, Z. Muhammad, W. S. Chu, Z. H. Wang, H. F. Xiang, Q. Liu, L. Song, *ACS Nano* **2017**, *11*, 6483.

[54] L. L. Wang, X. Z. Zhang, G. Z. Shen, X. Peng, M. Zhang, J. L. Xu, *Nanotechnology* **2016**, *27*, 095602.

[55] X. J. Zhao, G. Wang, Y. X. Zhou, H. Wang, *Energy* **2017**, *118*, 172.

[56] S. Yoon, S. Lee, S. Kim, K. W. Park, D. Cho, Y. J. Jeong, *J. Power Sources* **2015**, *279*, 495.

[57] J. Y. Ji, Y. Li, W. C. Peng, G. L. Zhang, F. B. Zhang, X. B. Fan, *Adv. Mater.* **2015**, *27*, 5264.

[58] X. L. Wang, G. Q. Shi, *Energy Environ. Sci.* **2015**, *8*, 790.

[59] W. Lv, Z. J. Li, Y. Q. Deng, Q. H. Yang, F. Y. Kang, *Energy Storage Mater.* **2016**, *2*, 107.

[60] H. X. Zhang, S. L. Jing, Y. J. Hu, H. Jiang, C. Z. Li, *J. Power Sources* **2016**, *307*, 214.

[61] Y. H. Dou, J. T. Xu, B. Y. Ruan, Q. N. Liu, Y. D. Pan, Z. Q. Sun, S. X. Dou, *Adv. Energy Mater.* **2016**, *6*, 1501835.

[62] Y. H. Yang, B. Wang, J. Y. Zhu, J. Zhou, Z. Xu, L. Fan, J. Zhu, R. Podila, A. M. Rao, B. G. Lu, *ACS Nano* **2016**, *10*, 5516.

[63] J. G. Wang, D. D. Jin, R. Zhou, X. Li, X. R. Liu, C. Shen, K. Y. Xie, B. H. Li, F. Y. Kang, B. Q. Wei, *ACS Nano* **2016**, *10*, 6227.

[64] S. K. Park, C. Y. Seong, S. Yoo, Y. Z. Piao, *Energy* **2016**, *99*, 266.

[65] L. David, R. Bhandavat, U. Barrera, G. Singh, *Nat. Commun.* **2016**, *7*, 10998.

[66] J. R. He, P. J. Li, W. Q. Lv, K. C. Wen, Y. F. Chen, W. L. Zhang, Y. R. Li, W. Qin, W. D. He, *Electrochim. Acta* **2016**, *215*, 12.

[67] Y. F. Chao, R. Jalili, Y. Ge, C. Y. Wang, T. Zheng, K. W. Shu, G. G. Wallace, *Adv. Funct. Mater.* **2017**, *27*, 1700234.

[68] X. Y. Wang, L. Fan, D. C. Gong, J. Zhu, Q. F. Zhang, B. G. Lu, *Adv. Funct. Mater.* **2016**, *26*, 1104.

[69] L. R. Shi, C. L. Pang, S. L. Chen, M. Z. Wang, K. X. Wang, Z. J. Tan, P. Gao, J. G. Ren, Y. Y. Huang, H. L. Peng, Z. F. Liu, *Nano Lett.* **2017**, *17*, 3681.

[70] T. C. Jiang, F. X. Bu, X. X. Feng, I. Shakir, G. L. Hao, Y. X. Xu, *ACS Nano* **2017**, *11*, 5140.

[71] T. Hoshide, Y. C. Zheng, J. Y. Hou, Z. Q. Wang, Q. W. Li, Z. G. Zhao, R. Z. Ma, T. Sasaki, F. X. Geng, *Nano Lett.* **2017**, *17*, 3543.

[72] T. C. Jiang, F. X. Bu, B. L. Liu, G. L. Hao, Y. X. Xu, *New J. Chem.* **2017**, *41*, 5121.

[73] C. J. Tang, J. X. Zhu, X. J. Wei, L. He, K. N. Zhao, C. Xu, L. Zhou, B. Wang, J. Z. Sheng, L. Q. Mai, *Energy Storage Mater.* **2017**, *7*, 152.

[74] R. W. Mo, D. Rooney, K. N. Sun, H. Y. Yang, *Nat. Commun.* **2017**, *8*, 13949.

[75] J. R. He, Q. Li, Y. F. Chen, C. Xu, K. R. Zhou, X. Q. Wang, W. L. Zhang, Y. R. Li, *Carbon* **2017**, *114*, 111.

[76] W. N. Ren, C. Wang, L. F. Lu, D. D. Li, C. W. Cheng, J. P. Liu, *J. Mater. Chem. A* **2013**, *1*, 13433.

[77] H. Long, T. L. Shi, H. Hu, S. L. Jiang, S. Xi, Z. R. Tang, *Sci. Rep.* **2014**, *4*, 7413.

[78] H. L. Yu, C. L. Zhu, K. Zhang, Y. J. Chen, C. Y. Li, P. Gao, P. P. Yang, Q. Y. Ouyang, *J. Mater. Chem. A* **2014**, *2*, 4551.

[79] M. S. Balogun, C. Li, Y. X. Zeng, M. H. Yu, Q. L. Wu, M. M. Wu, X. H. Lu, Y. X. Tong, *J. Power Sources* **2014**, *272*, 946.

[80] Y. P. Chen, B. R. Liu, W. Jiang, Q. Liu, J. Y. Liu, J. Wang, H. S. Zhang, X. Y. Jing, *J. Power Sources* **2015**, *300*, 132.

[81] X. Wei, W. H. Li, J. A. Shi, L. Gu, Y. Yu, *ACS Appl. Mater. Interfaces* **2015**, *7*, 27804.

[82] H. F. Zhang, W. N. Ren, C. W. Cheng, *Nanotechnology* **2015**, *26*, 274002.

[83] X. H. Wang, L. M. Sun, R. A. Susantyoko, Q. Zhang, *Carbon* **2016**, *98*, 504.

[84] S. Li, G. Liu, J. Liu, Y. K. Lu, Q. Yang, L. Y. Yang, H. R. Yang, S. L. Liu, M. Lei, M. Han, *J. Mater. Chem. A* **2016**, *4*, 6426.

[85] M. S. Balogun, Z. P. Wu, Y. Luo, W. T. Qiu, X. L. Fan, B. Long, M. Huang, P. Liu, Y. X. Tong, *J. Power Sources* **2016**, *308*, 7.

[86] S. H. Zhao, J. X. Guo, F. Jiang, Q. M. Su, G. H. Du, *Mater. Res. Bull.* **2016**, *79*, 22.

[87] X. H. Wang, M. Zhang, E. Liu, F. He, C. S. Shi, C. N. He, J. J. Li, N. Q. Zhao, *Appl. Surf. Sci.* **2016**, *390*, 350.

[88] Z. N. Deng, H. Jiang, Y. J. Hu, Y. Liu, L. Zhang, H. L. Liu, C. Z. Li, *Adv. Mater.* **2017**, *29*, 1603020.

[89] M. S. Balogun, M. H. Yu, C. Li, T. Zhai, Y. Liu, X. H. Lu, Y. X. Tong, *J. Mater. Chem. A* **2014**, *2*, 10825.

[90] W. W. Li, L. Gan, K. Guo, L. B. Ke, Y. Q. Wei, H. Q. Li, G. Z. Shen, T. Y. Zhai, *Nanoscale* **2016**, *8*, 8666.

[91] X. L. Wang, G. Li, M. H. Seo, G. Lui, F. M. Hassan, K. Feng, X. C. Xiao, Z. W. Chen, *ACS Appl. Mater. Interfaces* **2017**, *9*, 9551.

[92] L. F. Shen, Q. Che, H. S. Li, X. G. Zhang, *Adv. Funct. Mater.* **2014**, *24*, 2630.

[93] M. S. Balogun, M. H. Yu, Y. C. Huang, C. Li, P. P. Fang, Y. Liu, X. H. Lu, Y. X. Tong, *Nano Energy* **2015**, *11*, 348.

[94] S. Fang, L. F. Shen, P. Nie, G. Y. Xu, L. Yang, H. Zheng, X. G. Zhang, *Part. Part. Syst. Charact.* **2015**, *32*, 364.

[95] Y. Zhao, C. L. Ma, Y. Li, H. L. Chen, Z. P. Shao, *Carbon* **2015**, *95*, 494.

[96] X. Y. Wu, S. M. Li, B. Wang, J. H. Liu, M. Yu, *Phys. Chem. Chem. Phys.* **2016**, *18*, 4505.

[97] X. F. Wang, B. Liu, X. J. Hou, Q. F. Wang, W. W. Li, D. Chen, G. Z. Shen, *Nano Res.* **2014**, *7*, 1073.

[98] G. Q. Tan, F. Wu, Y. F. Yuan, R. J. Chen, T. Zhao, Y. Yao, J. Qian, J. R. Liu, Y. S. Ye, *Nat. Commun.* **2016**, *10*, 1038.

[99] B. Sun, K. Huang, X. Qi, X. L. Wei, J. X. Zhong, *Adv. Funct. Mater.* **2015**, *25*, 5633.

[100] X. Fang, C. F. Shen, M. Y. Ge, J. P. Rong, Y. H. Liu, A. Y. Zhang, F. Wei, C. W. Zhou, *Nano Energy* **2015**, *12*, 43.

[101] Y. H. Bao, X. Y. Zhang, X. Zhang, L. Yang, X. Y. Zhang, H. S. Chen, M. Yanga, D. N. Fang, *J. Power Sources* **2016**, *321*, 120.

[102] D. B. Kong, X. L. Li, Y. B. Zhang, X. Hai, B. Wang, X. Y. Qiu, Q. Song, Q. H. Yang, L. J. Zhi, *Energy Environ. Sci.* **2016**, *9*, 906.

[103] T. L. Gu, Z. Y. Cao, B. Q. Wei, *Adv. Energy Mater.* **2017**, *7*, 1700369.

[104] H. P. Wu, Q. H. Meng, Q. Yang, M. Zhang, K. Lu, Z. X. Wei, *Adv. Mater.* **2015**, *27*, 6504.

[105] Y. Zhang, Y. Z. Wang, Z. H. Xiong, Y. M. Hu, W. X. Song, Q. A. Huang, X. X. Cheng, L. Q. Chen, C. W. Sun, H. S. Gu, *ACS Omega* **2017**, *2*, 793.

[106] J. Liu, P. J. Lu, S. Q. Liang, J. Liu, W. J. Wang, M. Lei, S. S. Tang, Q. Yang, *Nano Energy* **2015**, *12*, 709.

[107] P. P. Sun, X. Y. Zhao, R. P. Chen, T. Chen, L. B. Ma, Q. Fan, H. L. Lu, Y. Hu, Z. X. Tie, Z. Jin, Q. Y. Xu, J. Liu, *Nanoscale* **2016**, *8*, 7408.

[108] D. L. Chao, X. H. Xia, J. L. Liu, Z. X. Fan, C. F. Ng, J. Y. Lin, H. Zhang, Z. X. Shen, H. J. Fan, *Adv. Mater.* **2014**, *26*, 5794.

[109] H. Xia, Q. Y. Xia, B. H. Lin, J. W. Zhu, J. K. Seo, Y. S. Meng, *Nano Energy* **2016**, *22*, 475.

[110] C. Wang, Y. H. Cao, Z. P. Luo, G. Z. Li, W. L. Xu, C. X. Xiong, G. Q. He, Y. D. Wang, S. Li, H. Liu, *Chem. Eng. J.* **2017**, *307*, 382.

[111] J. J. Bao, B. K. Zou, Q. Cheng, Y. P. Huang, F. Wu, G. W. Xu, C. H. Chen, *J. Membr. Sci.* **2017**, *541*, 633.

[112] J. Wang, L. Zhang, Q. W. Zhou, W. L. Wu, C. Zhu, Z. Q. Liu, S. Z. Chang, J. Pu, H. G. Zhang, *Electrochim. Acta* **2017**, *237*, 119.

[113] H. P. Wu, S. A. Shevlin, Q. H. Meng, W. Guo, Y. N. Meng, K. Lu, Z. X. Wei, Z. X. Guo, *Adv. Mater.* **2014**, *26*, 3338.

[114] Y. Lu, Q. Zhao, L. C. Miao, Z. L. Tao, Z. Q. Niu, J. Chen, *J. Phys. Chem. C* **2017**, *121*, 14498.

[115] E. H. Kil, K. H. Choi, H. J. Ha, S. Xu, J. A. Rogers, M. R. Kim, Y. G. Lee, K. M. Kim, K. Y. Cho, S. Y. Lee, *Adv. Mater.* **2013**, *25*, 1395.

[116] X. G. Ma, X. L. Huang, J. D. Gao, S. Zhang, Z. H. Deng, J. S. Suo, *Electrochim. Acta* **2014**, *115*, 216.

[117] Q. J. Wang, W. L. Song, L. Z. Fan, Q. Shi, *J. Power Sources* **2015**, *279*, 405.

[118] X. G. Ma, X. L. Huang, J. D. Gao, S. Zhang, Z. L. Peng, Z. H. Deng, J. S. Suo, *J. Power Sources* **2014**, *272*, 259.

[119] Q. F. Wang, B. Zhang, J. J. Zhang, Y. Yu, P. Hu, C. J. Zhang, G. L. Ding, Z. H. Liu, C. Z. Zong, G. L. Cui, *Electrochim. Acta* **2015**, *157*, 191.

[120] K. H. Choi, S. J. Cho, S. H. Kim, Y. H. Kwon, J. Y. Kim, S. Y. Lee, *Adv. Funct. Mater.* **2014**, *24*, 44.

[121] J. X. Zhang, N. Zhao, M. Zhang, Y. Q. Li, P. K. Chu, X. X. Guo, Z. F. Di, X. Wang, H. Li, *Nano Energy* **2016**, *28*, 447.

[122] H. Zhang, C. M. Li, M. Piszcz, E. Coya, T. Rojo, L. M. Rodriguez-Martinez, M. Armand, Z. B. Zhou, *Chem. Soc. Rev.* **2017**, *46*, 797.

[123] L. B. Hu, H. Wu, F. L. Mantia, Y. Yang, Y. Cui, *ACS Nano* **2010**, *4*, 5843.

[124] S. Leijonmarck, A. Cornell, G. Lindbergh, L. Wågberg, *J. Mater. Chem. A* **2013**, *1*, 4671.

[125] Q. H. Wang, S. W. Zhong, J. W. Hu, T. Liu, X. Y. Zhu, J. Chen, Y. Y. Hong, Z. P. Wu, *J. Power Sources* **2016**, *310*, 70.

[126] M. Park, H. Cha, Y. Lee, J. Hong, S. Y. Kim, J. Cho, *Adv. Mater.* **2017**, *29*, 1605773.

[127] A. M. Gaikwad, A. C. Arias, D. A. Steingart, *Energy Technol.* **2015**, *3*, 305.

[128] M. S. Balogun, Y. X. Zeng, W. T. Qiu, Y. Luo, A. Onasanya, T. K. Olaniyi, Y. X. Tong, *J. Mater. Chem. A* **2016**, *4*, 9844.

[129] M. S. Balogun, Y. Luo, F. Y. Lyu, F. X. Wang, H. Yang, H. B. Li, C. L. Liang, M. Huang, Y. C. Huang, Y. X. Tong, *ACS Appl. Mater. Interfaces* **2016**, *8*, 9733.

[130] M. S. Balogun, W. T. Qiu, F. Y. Lyu, Y. Luo, H. Meng, J. T. Li, W. J. Mai, L. Q. Mai, Y. X. Tong, *Nano Energy* **2016**, *26*, 446.

[131] M. S. Balogun, W. T. Qiu, J. H. Jian, Y. C. Huang, Y. Luo, H. Yang, C. L. Liang, X. H. Lu, Y. X. Tong, *ACS Appl. Mater. Interfaces* **2015**, *7*, 23205.

[132] W. Weng, Q. Sun, Y. Zhang, H. J. Lin, J. Ren, X. Lu, M. Wang, H. S. Peng, *Nano Lett.* **2014**, *14*, 3432.

[133] S. Xu, Y. H. Zhang, J. Cho, J. Lee, X. Huang, L. Jia, J. A. Fan, Y. Su, J. Su, H. G. Zhang, H. Y. Cheng, B. W. Lu, C. J. Yu, C. Chuang, T. Kim, T. Song, K. Shigeta, S. Kang, C. Dagdeviren, I. Petrov, P. V. Braun, Y. G. Huang, U. Paik, J. A. Rogers, *Nat. Commun.* **2013**, *4*, 1543.

[134] Y. B. Yin, X. Y. Yang, Z. W. Chang, Y. H. Zhu, T. Liu, J. M. Yan, Q. Jiang, *Adv. Mater.* **2017**, *29*, 1700378.

[135] T. Liu, J. J. Xu, Q. C. Liu, Z. W. Chang, Y. B. Yin, X. Y. Yang, X. B. Zhang, *Small* **2017**, *13*, 1602952.

[136] Q. C. Liu, T. Liu, D. P. Liu, Z. J. Li, X. B. Zhang, Y. Zhang, *Adv. Mater.* **2016**, *28*, 8413.

[137] Y. B. Yin, J. J. Xu, Q. C. Liu, X. B. Zhang, *Adv. Mater.* **2016**, *28*, 7494.

[138] T. Liu, Q. C. Liu, J. J. Xu, X. B. Zhang, *Small* **2016**, *12*, 3101.